

Abstract

ABDEL-KHALIK, HANY SAMY. **Inverse Method Applied to Adaptive**

Core Simulation. (Under the direction of Paul J. Turinsky).

The work presented in this thesis is a part of an ongoing research project conducted to gain insight into the applicability of inverse methods to developing adaptive simulation capabilities for core physics problems. Adaptive simulation is a simulation that utilizes past and current reactor measurements of reactor observables (*e.g.* core reactivity and incore instrumentation readings) to adapt the simulation in a meaningful way to improve agreement with reactor observables. To perform such adaption, we utilize a group of mathematical techniques which address the problem of given a current core simulator model and the associated input data (*e.g.* cross-sections, thermal-hydraulic parameters), how should the values of selected input data be adjusted to improve agreement with observables without changing the core simulator model, (*i.e.* how can we obtain the best agreement utilizing our current modeling capability). This is usually referred to as an inverse problem, which is difficult to solve due to its ill-posedness nature. Major advances have been made by mathematicians to overcome the ill-posedness nature of such problems. The proposed project is of an exploratory nature serving to develop expertise in this area, to which the nuclear power community has not participated to any great extent over the last two decades since their earlier contribution during the design, research and developments stages of a proto-typical fast breeder reactor. Exploratory research projects, such as this one, serve to develop insight, form general ideas about areas

where little expertise is available, and to provide a basis on whether there is potential for the proposed techniques to be useful and successful.

The current work addresses BWR core simulators since their prediction accuracy is inferior to PWRs', providing marginally acceptable agreement between measured and predicted core attributes. This implies that BWRs could benefit from utilizing an adaptive simulation tool. In the work done so far, a virtual approach has been utilized in which two versions of a core simulator (*i.e.* FORMOSA-B) are utilized. The first one represents actual plant data, and is referred to as the 'virtual core'. In that version, the LPRM readings and their associated instrumental noise have been simulated. The second one is an altered version of the same core simulator, in which modeling and input data errors are introduced to give rise to disagreement between the two versions of the core simulator, and is referred to as the 'design basis core simulator'. That disagreement is made to be of the same magnitude as the actual disagreement which exists between plant data and current core simulators in regard to LPRM readings and core criticality. The virtual core observables at nominal conditions, including the noise component of the LPRM readings, are then utilized to adapt the design basis core simulator. A larger set of virtual core observables including those at nominal and various off-nominal core conditions, with and without the noise signal, is then contrasted to those predicted by the 'adapted design basis core simulator'. Results indicate that the disagreement between the adapted design basis core simulator and the virtual core can be decreased by an order of magnitude, indicating the high fidelity and robustness of the adaptive techniques and that adaption can be utilized as an effective noise filter. These favorable results encourage further development

of this project. If successful in improving prediction fidelity when utilizing actual plant data as the basis for adaption, this could lead to an increase in design margins and relaxing of technical specifications, which will have a beneficial impact on reactor operation and economy.

Inverse Method Applied to Adaptive Core Simulation

by

Hany Samy Abdel-Khalik

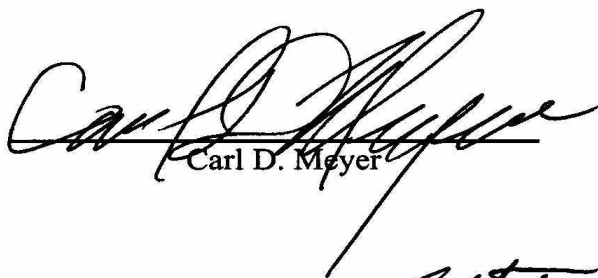
A thesis submitted to the Graduate Faculty of
North Carolina State University
in partial fulfillment of the
requirements of the Degree of
Master of Science

Nuclear Engineering

Raleigh, North Carolina

2002

APPROVED BY:

A handwritten signature in black ink, appearing to read 'Carl D. Meyer', written over a horizontal line.

Carl D. Meyer

A handwritten signature in black ink, appearing to read 'Anistratov', written over a horizontal line.
Dmitriy Y. AnistratovA handwritten signature in black ink, appearing to read 'Paul J. Turinsky', written over a horizontal line.
Paul J. Turinsky, Chair of Advisory Committee

‘Wisdom lies in Truth’

I dedicate this work to anyone who might benefit from it.

Biography¹

Hany S. Abdel-Khalik was born in Alexandria, Egypt on July 15th, 1978. He is the oldest of the five children of Samy I. Abdel-Khalik and Yousria M. Nourel-Deen. He received his elementary education locally, graduating from Gamal Abdel-Naser High School in 1995. He received his Bachelor of Science from Alexandria University in July 2000 from the department of Nuclear Engineering and he was the college valedictorian that year. He was looking forward to continuing his graduate studies in the area of reactor physics. Upon graduation, he had the wonderful opportunity to join the Electric Power Research Center at North Carolina State University as a research assistant. Since the fall of 2000 he has been working under the supervision of Dr. Paul J. Turinsky. He will continue his work on the project proposed in this thesis as a part of his PhD work. Hany holds the ANS Allan F. Henry/Paul A. Greebler graduate scholarship, and is a recipient of the ANS Reactor Physics Division best paper award at the Summer 2002 ANS national meeting.

1. The author may be contacted at:
Address: 1222 Burlington Labs,
North Carolina State University,
P. O. Box 7909,
Raleigh, NC 27695-7909,
USA.
Email: hsabdelk@ncsu.edu

Acknowledgements

I would like to say thank you to many wonderful people in this very short space. First, I thank my parents for their continuous support and strong will to provide for me the best life possible. I also thank my siblings for their enormous love and self-sacrifice for me. Dr. Mohamed E. Nagy has supported and encouraged me during my undergraduate study, and to him I am indebted. I would like to thank my advisor Dr. Paul J. Turinsky for giving me the chance to work on this wonderful project. His patience and support through the first two years of my graduate study are very well appreciated. His innovative ideas were among the main reason we won the ANS RPD best paper award. I have enjoyed the insightful and intuitive discussions with Dr. Dmitriy Y. Anistratov and Dr. Carl D. Meyer. I am very thankful to my uncle Dr. Said I. Abdel-Khalik; he has given me unconditional support and care. His wife Sharon has given me invaluable advice. Finally, I thank Dr. Youssef A. Shatilla for his recommendations and advice throughout my graduate and undergraduate studies.

Table of Contents

List of Tables	vii
List of Figures	viii
Nomenclature	x
1. Adaptive Core Simulation	1
1.1. Importance to Advanced and Current Reactors	1
1.2. Description of Core Simulators	3
1.3. Sources of Simulation Errors	4
1.4. Adaptive Simulation Approach (Main Assumptions)	5
1.5. Previous Development and Motivation for Adaptive Techniques	6
1.6. Current Practice	8
1.7. Inverse Problem	10
1.7.1 Definition and Areas of Application	10
1.7.2 Mathematical Description	12
1.7.3 Ill-Posed Problems	14
1.7.4 Regularization of Ill-Posed Problems	15
1.8. Scope of Work	16
2. Virtual Approach	17
2.1. Description of the Virtual Approach	17
2.2. Advantages of Virtual Approach Utilization	18
2.3. Core Parameterization	18
2.3.1 Thermal-Hydraulics Core Parameterization (Simulation of Modeling Errors)	19
2.3.2 Reactor Physics Core Parameterization	20
2.4. Simulation of Input Data Errors	23
3. Discrete Inverse Theory	27
3.1. Objective	27
3.2. Definitions	28
3.2.1 Parameter Space	28
3.2.2 Data (Observables) Space	29
3.2.3 Linear Transformation	29
3.2.4 SVD Decomposition	30
3.2.5 Anatomy of Linear Transformation	32
3.2.6 Reverse Transformation	33
3.2.7 Inverse Transformation	35

3.2.8	Ill-posedness and Ill-conditioning	36
3.2.9	Forward Problem	39
3.2.10	Inverse Problem	39
3.2.11	Measure of Distance	39
3.2.12	Best Approximation	41
3.2.13	Inner Product and Orthogonality	43
3.3.	Adapting the Core Simulator Model	46
3.3.1	Model Linearization	47
3.3.2	Least-Squares Approach	48
3.3.3	Geometrical Interpretation of Least-Squares Solution and Its Deficiencies . .	50
3.3.4	Sources and Consequences of Ill-Conditioning	52
3.3.5	Regularized Least Squares Problem	54
3.3.6	Determination of the Regularization Parameters and Weighting Matrices . .	56
3.3.7	Tuning of Adaptive Techniques	58
4.	Cases Studied, Results and Conclusions	60
5.	Future Work and Recommendations	79
	References	83
	Appendices	88
A.	Data Information Content	89
B.	Tikhonov Regularization	91

List of Tables

Table 2.1: Isotopics treated in the core simulator model.	21
Table 2.2: Selected set of adjusted microscopic cross-sections.	21
Table 4.3: Figures' nomenclature.	63

List of Figures

Figure 3.1: Mapping Information between Parameters and Data Spaces.	34
Figure 3.2: Notion of Best Approximation.	42
Figure 3.3: Projection of the Measured Observables onto the Linearized Core Model (Different $\bar{\Lambda}$ Matrices).	46
Figure 3.4: Inverse Mapping of Information in a ‘Discrete Ill-Posed System’.....	53
Figure 3.5: Supplying A Priori Information about Model Parameters.	56
Figure 4.1: Detectors’ Layout.	61
Figure 4.2: Control Rod Pattern For Core Follow Data.	71
Figure 4.3: Detectors’ Signals Mismatch & Core Reactivity Error (Rated Conditions). 72	
Figure 4.4: Simulated Core Follow Data at Rated Conditions, High Void and Low Void.	73
Figure 4.5: Detectors’ Signals Mismatch & Core Reactivity Error (High Void Fraction).	74
Figure 4.6: Detectors’ Signals Mismatch & Core Reactivity Error (Low Void Fraction).....	75
Figure 4.7: Detectors’ Signals Mismatch & Core Reactivity Errors (Different Criteria).	76
Figure 4.8: Detectors’ Signal Mismatch & Core Reactivity Errors.....	77
Figure 4.9: A Posteriori and A Priori Information About Model Parameters	78
Figure 5.1: Road Map for Adaptive Core Simulation Project	82
Figure B.1: L-Curve, ‘A Posteriori Information about Model Parameters and	

Core Observables'	94
Figure B.2: Effect of Regularization on the Conditioning of the	
Unconstrained Least-Squares Problem	96
Figure B.3: L-Curve for a Single Iteration Unconstrained Search	97

Nomenclature

Acronyms:

AC	Adapted Design Basis Core Simulator.
BOC	Beginning Of Cycle.
BWR	Boiling Water Reactor.
CRH	Control Rod History.
CRD	Control Rod Insertion Branch Case.
DC	Design Basis Core Simulator.
EOC	End Of Cycle.
FP	Fission Products Branch Case.
HFP	Hot Full Power.
LPRM	Local Power Range Monitors.
MWD	Mega-Watt-Day
PWR	Pressurized Water Reactor.
RMS	Root Mean Square.
REF	REFERENCE or Base Depletion Case.
STU	Short-Tonnes-U, STU=1.1023113 MTU.
TIP	Traveling Incore Probe.
TF	Fuel Temperature Branch Case.
VC	Virtual Core.

Physical Symbols:

C_0	Void-quality concentration parameter.
k_3	Void-quality terminal velocity parameter.
ρ_g	Density of the vapor phase.
ρ_g	Density of the liquid phase.
α	Void fraction.
x	Flow quality.
G	Coolant mass flux.
σ	Surface tension, microscopic cross-section or standard deviation.
V_{gj}	Void-quality drift velocity parameter.
g	Gravitational acceleration constant.
k_{eff}	Core criticality eigenvalue.
σ_{a1}	Microscopic fast absorption cross-section.
σ_{a2}	Microscopic thermal absorption cross-section.
σ_{f1}	Microscopic fast fission cross-section.
σ_{f2}	Microscopic thermal fission cross-section.
ν	Number of neutrons emitted per fission.
κ	Energy emitted per fission.

Variables' Notations:

k	Iterate number, (<i>i.e.</i> p_k).
m	Measured Observables, (<i>i.e.</i> \vec{d}^m).
c	Calculated (<i>e.g.</i> predicted) Observables, (<i>i.e.</i> \vec{d}^c).
$*$	Scalar quantity.
$\vec{*}$	Vector quantity.
$\overset{=}{*}$	Matrix Operator.

1. Adaptive Core Simulation

1.1. Importance to Advanced and Current Reactors

The accurate prediction of core behaviour is a fundamental requirement to the design and operation of any nuclear reactor system. That is achieved through the utilization of high fidelity core simulators. Core simulators can be utilized in either an on-line or off-line mode. In the online mode, they provide support for the successful control and protection of the reactor. Control systems are required to determine the optimum trajectory in moving the reactor from the current state to a final desired state with all operational and safety limits satisfied. Protection systems are required to be capable of determining current and near-term reactor states for a range of reactor conditions to advise reactor operators, or to automatically activate safety systems to help take the appropriate actions to avoid and/or mitigate any accident scenarios. Off-line core simulators are also as important during the design as well as operational phases of the plant to determine the optimum operating core conditions (*i.e.* fuel loading pattern, control rod programming, etc.). They are also utilized to interpret experimental results.

The quality of core simulators' predictions will impact the reactor economy through the introduction of design margins on the core design to ensure an operation, in which the safety and operational limits are satisfied[1]. How tight or relaxed these margins are depends on how accurate the predictions of core behaviour are. The uncertainties of core simulators' calculations are thus very crucial to the determination of these margins. Large uncertainties will result in diminishing core design freedom and hence adversely impact economics. On the other hand, any reduction in these uncertainties will beneficially impact different aspects of

reactor economy such as reducing fuel and/or operating cost or even initial capital investment for a new plant. By way of a few examples[2]: 1) By accurately calculating thermal limits, one can reduce thermal margins, and be able to operate the reactor at higher power densities which is economically more favorable (operating cost reduction). That translates into smaller sized cores for new reactors (reduction in capital investment). 2) With more accurate calculations of core reactivity for various states, one may be able to reduce the number of control rods (reduction in capital investment), or reduce the U^{235} enrichment margin required in the fresh fuel for the core to reach the desired cycle life at the desired rated power (reduction in fuel cost).

High fidelity core simulators are hence essential components for any reactor system during the design and/or the operational phases. To achieve, in the near term, this high level of fidelity, dictated by economic, operational and safety considerations, will require high fidelity and robust adaptive techniques[3]. Adaptive simulation techniques utilize past and current reactor measurements of reactor observables to adapt the simulation in a meaningful way to improve agreement with observable values. Fidelity denotes the ability of an adapted simulator to accurately predict the measured observables. Robustness denotes the ability of the adapted simulator to accurately predict measured core attributes which are not directly observed, for example, the measured observables recorded at future times; and the observables for core conditions that differ from those at which adaption is completed. Adaptive simulation can also be useful in establishing a basis for deciding where future experimental efforts should be focused to decrease core attributes' uncertainties. That can be achieved by contrasting the core parameters' adjusted values versus their current known values, along with knowledge of

the impact their adjusted values will have on different core attributes, the costs associated with uncertainties on these core attributes, and the costs of experiments to reduce core attributes' uncertainties. The need for adaptive simulation is viewed to be greater for Generation IV versus Generation II and III reactors, since limited applicable experience will be available for Generation IV reactors. Adaptive simulation can also be used to effectively interpret experimental results done in the course of developing Generation IV reactors, help determine the major causes of discrepancies between predicted and measured values, and hence help direct how the experimental program should be designed to reduce the uncertainties in the evaluation of the important parameters.

1.2. Description of Core Simulators

The behaviour of a nuclear reactor core is governed by the neutron flux distribution in space, energy and time. One of the central problems of core simulation models is to accurately predict this distribution. The core simulator model consists of models for both reactor physics and thermal-hydraulics, which is necessary to account for the non-linear feedback mechanisms through cross-sections. Typically, reactor physics behavior is modeled employing few-group neutron diffusion theory, hydraulics behaviour is modeled employing some 1-D approximate form of the Navier-Stokes equations (*e.g.* drift flux model), and the thermal behavior is modeled using some approximate thermal model (*e.g.* functionalizing fuel temperature as a function of linear power density).

Input data to the core simulator are enormous and determined by the needs of the models employed within. Note that we include in input data, the coefficients that appear in various correlations, including the thermal-hydraulic correlations. This follows since core

thermal-hydraulic simulations require user input of core geometry as well as many empirical parameters, such as local form loss coefficients and heat transfer coefficients. The input data to the core simulator, in many cases, are determined using computer codes that model aspects of the core physics in more detail than the core simulator models do, such as with the determination of few-group homogenized cross-sections using lattice physics codes. So, in general, the input data include any data directly passed to the core simulator or indirectly through any preprocessor code.

Core observables include the readings of incore detectors (*e.g.* LPRMs and TIPs), which are usually positioned throughout the core in between flow channels which do not have control rods. Since core simulators are usually based on a steady state model and measured observables are normally taken at steady state conditions, core reactivity could also serve as a basis for adaption (*e.g.* $k_{eff} = 1$ at all times).

1.3. Sources of Simulation Errors

Core simulators introduce errors in the predicted core attributes, including core observables, due to input data and computational (*e.g.* modeling) errors. Input data (*e.g.* cross-sections and thermal-hydraulic parameters), whether they are experimentally measured or theoretically calculated, contain uncertainties associated with their evaluation which are described by standard deviation values reported as part of the data evaluation process. Modeling errors occur due to different reasons: 1) The common practice in modeling is to avoid sophistication by introducing approximations in the mathematical description to simplify the treatment, that results in the introduction of errors in the calculations (*i.e.*

diffusion versus transport theory calculations for the whole core). 2) Inadequacies in the mathematical model utilized for simulating the core (*e.g.* failure to present all aspects of the physics governing the core behaviour). 3) Numerical solution techniques' approximations (*i.e.* spatial domain discretization).

The pre-processing codes also introduce errors into the core simulator's input data, hence into the core simulator's predictions of core attributes. This follows since, just like the core simulator, errors exist in the input data to the pre-processor codes, in the mathematical models of the physics, and in the numerical solution techniques employed in these codes.

Computational methods and input data uncertainties have always been the sources of the limitation of nuclear calculations. In some instances, the computational uncertainties dominate the sources of discrepancies, however, over the last few decades computational methods have reached a stage of maturity in their sophistication and applicability. Computational power has also increased considerably enabling the solution of bigger problems in relatively shorter computer execution times. With the current status of models' sophistication and huge experience obtained from power plants' operations, we believe that more attention should be directed towards input data errors and show how these data can be adjusted using measured plant data to effectively reduce the disagreement between the measured (*e.g.* core observables) and predicted core attributes.

1.4. Adaptive Simulation Approach (Main Assumptions)

Adaptive simulation is a mathematical algorithm which deals with given a mathematical model of certain physical phenomena and the associated input (model parameters) and output (measured observables) data of the model, how can one adjust the

input data, without adjusting the model, to reduce the disagreement between the measured and predicted observables. The sources for the disagreement are either due to noise in the measured output or simulation errors which, as described before, consist of modeling and input data errors. Accordingly, it will be assumed that the dominant sources of errors in predicted core attributes, including the core observables, originate due to errors in the input data to the pre-processor codes and pre-processor codes' independent input data to the core simulator. That implies that input data will be adapted (*e.g.* adjusted) to improve the agreement between predicted and measured observables, even though components of the sources of disagreement are due to both input data and modeling errors. This assumption is likely valid and also necessary in order to avoid the issue of simultaneous adaptation of the core simulator's models, since the combined adaptation problem of core simulator's input data and models is beyond current and foreseeable capabilities. However, a justification for that assumption has to be investigated in this study by checking the fidelity and robustness of the adaption.

1.5. Previous Development and Motivation for Adaptive Techniques

The art of data adjustment had been used extensively during the 1970s for fast reactors' experimentation. The data selected for adjustment were the cross-sections obtained from differential experiments. The uncertainty level of the differential experiments' evaluated cross-sections did not meet the requirement for an accurate description of certain integral core parameters, (*i.e.* breeding ratio[4] or k_{eff} eigenvalue). Uncertainty in the basic cross-section data affects the uncertainty of the core integral parameters, which necessitate the introduction of more uncertainty allowances in the design of different components of the reactor. These

allowances result in cost increases and reduction from optimum core performance. Integral experiments' results were used in conjunction with differential experiments to adjust cross-sections, in a hope that this will reduce the important core parameters' uncertainties[5] . Integral experiments are typically critical assemblies operating at zero power, in which a small-scale mock-up of the large-scale core is built to mimic the reactor core behaviour as much as possible in regards to composition and geometry.

The idea for the proposed work of adaptive core simulation stems from these past experiences[6]-[11]; but, with two major differences: The first is that instead of using small scale experiments to simulate the operation of the real reactor, one can use the full-scale experiment, (*e.g.* real core), as one's integral experiment. This is advantageous when considering the huge amount of core follow data from our operating experience with current power plants. However, the interpretation of these data is much more complex than the "clean" integral experiments, since the quality of the data is uneven. For integral experiments, the quality of the data is considered to be the same, since there are no depletion effects and no thermal-hydraulic feed-back effects. However for a power plant, these effects are present, transient phenomena might be occurring at anytime yet a steady state core model is employed, and instrumentation may not be properly calibrated or failed. Those are examples of such difficulties one might encounter when interpreting plant data.

The second difference is in the mathematical formulation of the problem. The problem at hand can be treated as an "inverse problem", which is an extremely difficult problem. However, over the last four decades, since the early papers by Tikhonov in 1963[12]-[13], inverse methods have been extensively developed on a solid mathematical basis and have been applied to many engineering areas, specifically, the image enhancement community has

advanced considerably using powerful inverse methods[14]. The nuclear power community however has not participated to any great extent in these activities, in spite of their earlier significant participation in the data adjustment area.

There are different issues and concerns that need to be analyzed when adjusting input data. Reliability of the adjusted data denotes how well they will perform at different core conditions and how consistent they are with the unadjusted data[15]. Uniqueness of the adjustments denotes, would one obtain the same results if one starts from two different data sets utilizing the same measured observables to adapt the core simulator? This type of analysis can also help answer some other questions such as: 1) How well do the existing cross-section or thermal-hydraulic data predict the core attributes of interest with the current modeling capabilities? 2) How sensitive are certain core attributes to changes in the data, (*i.e.* use of an alternative cross-section data set)? 3) How does one identify the sources/causes of discrepancies between the core simulator's predicted and measured core attributes? Answering question (3) will provide direction to those areas of uncertainty where more detailed experimental programs are required.

As a preable to the following discussion, note that the adaption approach we are proposing to develop is for off-line application utilizing the observable data from many different sources, including different reload cycles for the same nuclear power plant, different nuclear power plants of the same type, and ultimately different types of nuclear power plants.

1.6. Current Practice

Very limited or no adaption is employed in current on-line core simulators, completed in a way which is conceptually different from what is proposed in this study. The differences

between measurements and predictions are usually fitted using surface response methodologies and are used to predict the discrepancy between future predictions and measurements. Similar versions of this approach were utilized during the course of fast reactors experiments, and are referred to as “bias factor methods”[16]. The “bias operator method” is another mathematically elegant tool that has also been proposed in the past as a method for adaption[17]-[20]. Neither of these methods will be utilized in our work, since we believe they do not have a physical justification. In the proposed work, however, the adjustments are done to the input data in a mathematically consistent way in which the physics of the problem is satisfied. That is achieved by first limiting the input data adjustments by the uncertainty information, sometimes propagated through the pre-processors’ codes to the core simulator to preserve the proper pre-processor codes’ core physics behaviour. In doing so, the proposed adjustments will be consistent with their known uncertainties. Second, the input data adjustments will be propagated through the core model satisfying the physics described by the core simulator. Physical justification is required when adapting core input data, since if the physics of the core are not satisfied, one would not be able to predict core behaviour at different operating conditions than those adapted to, defeating the whole purpose of the adaption. Third, the uncertainties in the core observables will be accounted for during the adaption, assuming that the input data adjustments are consistent with the quality of the experimental core observables being adjusted to.

1.7. Inverse Problem

1.7.1 Definition and Areas of Application

From a mathematical point of view, the definitions of a direct problem and an inverse problem are always ambiguous. This can be well illustrated by a frequently quoted statement of J. B. Keller[22]: *“We call two problems inverses of one another if the formulation of each involves all or part of the solution of the other. Often, for historical reasons, one of the two problems has been studied extensively for some time, while the other has never been studied and is not so well understood. In such cases, the former is called the direct problem, while the latter is the inverse problem.”* So one of the two problems has been studied well, and the physical model used to describe it is well understood and has been justified by experiments, and usually is considered to be more fundamental than the other problem.

The notion of direct and inverse problems in engineering however can be described in a more straightforward way[14],[21]. A forward problem can be defined to be the process in which data are the output of some physical model, whose input are some physical parameters. However, an inverse problem is one in which we are interested in estimating those parameters on which the model depends, based on a prior knowledge of the data (the output of the forward problem). From an experimental point of view, usually data are collected from any system, to gain more information about the behaviour of that system, and if these data can be described by a certain model we can predict the behaviour of that system under different conditions. However, what we are interested in knowing is usually different from what we measure, so, if we can use our mathematical model to extract information about what we want from the data we have, we call that an inverse problem. The model's parameters (the

unknowns) are the quantities that one is trying to estimate. The matter of how to choose these parameters is usually problem dependent and quite often somewhat arbitrary. The inverse problem is however less suited to provide the fundamental mathematics or physics of the model itself. The main role of the theory is to infer numerical information about unknown parameters of the model and not the type of the model itself; so a good idea of the applicable forward model must be available in order to take advantage of the inverse theory. For example, inverse theory can not suggest a new void-quality equation form to calculate the amount of voiding in a BWR core; however it can determine the best values for the parameters associated with a given void-quality evaluation form. Possible goals of an inverse analysis might include 1) estimates of a set of model parameters, 2) estimates of the bounds on the range or acceptable model parameters, 3) estimates of the formal uncertainties in the model parameters, 4) sensitivity of the solution to noise (or small change) in the data, 5) determination of the best set of data suited to estimate a certain set of model parameters, 6) the adequacy of the fit between the predicted and observed data, and 7) directions to decide whether a more sophisticated model will be significantly better than a more simple one or not. All these goals emphasize that inverse theory is not just used to determine the optimum values for model parameters but also provides different criteria by which the quality of those estimated parameters can be judged. It is to be noted, however, that a solution to an inverse problem might contain not a “single” answer like a forward problem, so one of the parts of the inverse analysis is the ability to determine which answer is reasonable, valid, and acceptable.

Inverse theory has found many applications in many different branches of physical sciences, such as: (a) image enhancement, (b) geophysical applications, like earth structure

and earthquake location determination, (c) satellite navigation, (d) molecular structure by x-ray diffraction, and (e) medical tomography.

1.7.2 Mathematical Description

Inverse theory has been developed over the past four decades by scientists and mathematicians having various backgrounds. This has resulted in presenting the theory in many different ways[21], tending to superficially look very different in spite of the strong and fundamental similarities that exist between them. Inverse theory can be derived from (1) pure statistical concepts, (*i.e.* Bayesian decision analysis, and information content concepts), or from more (2) deterministic ways which avoids mentioning terms like probability distribution and prefer terms like inverse transformation, (*i.e.* minimum variance approaches). Inverse theory can also be classified according to the type of both the model parameters and the observed data by whether they are continuous functions or discrete values. The problem we are interested in is a discrete-discrete problem, which means that both the data and the parameter space are discrete or finite dimensional spaces. This will make our mathematical analysis much easier than the general inverse theory. The reasons behind the finite dimensionality of our problem is that our observables are instrument readings, and the parameters we are looking for are ones associated with the thermal-hydraulic and reactor physics model, (*e.g.* thermal property constants and cross-sections).

A discrete inverse problem is much simpler than the continuous one, since the mathematical vehicle needed for the discrete case is linear algebra, and ideas like vector spaces and matrix representation of linear transformations are sufficient to fully describe the problem. In fact, discrete inverse theory can be fully described in terms of optimization

techniques by vector space methods[23],[24]. For the continuous case, the problem gets much more complicated and more abstract elements from the theory of functional analysis are needed to describe the problem. Functional analysis abstracts our intuition about geometry of ordinary vector spaces by merging linear algebra and analysis. The functional analysis approach reveals itself to be tremendously more powerful and elegant than the linear algebra approach. That leads some readers to hope that these elegant tools might help solve much more complicated problems beyond the reach of the simple mathematical analysis provided by linear algebra. Unfortunately, realization of such hopes is rarely encountered in practice. The primary role of functional analysis is to unify and abstract our simple ideas about vector spaces in a more mathematical and rigorous fashion.

In general, inverse theory can be described in a continuous form and then the special discretization for the specific problem of interest can subsequently be introduced[25],[26]. However, since the problem of interest is a discrete one, the fully mathematical rigorous treatment of the continuous inverse problem will be considered to be beyond the scope of this work, and only the discrete inverse problem will be presented.

Inverse problems can be either under or over-determined. For the core simulator[3], the problem is under-determined in that there are many more input data items that can be adjusted than there are observables. Parametrization of the system is one way to recast the problem from an under to over-determined one. Parametrization, within the context of our application, is the process of characterizing core simulator data in terms of a minimal set of parameters, which we shall refer to as core parameters. Care is required in the selection of those parameters since improper choices made will be reflected in poorer fidelity and/or robustness of the adaptive simulator. One can then think of utilizing a weighted least squares

approach to determine the unknown core parameters, so as to minimize the differences in the predicted and measured values of the observables. The weights can be selected to reflect the uncertainties in both the observables and input data. This least squares problem will likely be ill-posed or at least ill-conditioned.

1.7.3 Ill-Posed Problems

A problem is said to be ill-posed if it is not well-posed. According to the french mathematician Jacques Hadamard[27], for a problem to be well-posed, the following three conditions, within the context of the current application, must exist: 1) There is a solution for the core parameters. 2) The solution for the core parameters is unique. 3) The values of core parameters change smoothly with smooth changes in the values of the observables. Item (1) or Item (2) if not satisfied is obviously troublesome in that either no or a non-unique solution for the core parameters exists. Item (3) if not satisfied is troublesome since it implies that the values of core parameters are highly sensitive to the values of observables. Given that observables contain experimental errors, one cannot tolerate the high sensitivity associated with Item (3). This item also has implications with regard to robustness of adaptation. The mathematical distinction between a well- and an ill-posed problem is very clear. However, in practice, when considering the discretization of the problem and the associated errors (noise) in the measured observables, that distinction reveals itself to be less apparent. In some cases, one cannot obtain an accurate, unique solution for a well-posed problem due to the finite precision of the computations, forcing us to treat such problems as ill-posed. Further details about such issues will be introduced in the next chapter.

1.7.4 Regularization of Ill-Posed Problems

In Hadamard's opinion, an ill-posed problem does not have a physical meaning. However, it turns out that an ill-posed problem can be extended to a well-posed one. That extension is usually obtained by recognizing that the information supplied by the observables about model parameters is not sufficient to give rise to a well-posed problem. Regularization refers to the mathematical methods utilized to incorporate extra information about model parameters necessary to recast an ill-posed problem into a well-posed one. An ill-posed problem is regularized by either altering the mathematical model of the physical processes or by restricting the space of the solutions allowed. The first technique of altering the mathematical model will not be addressed in this study, since the intention is to enhance the current models' prediction accuracies without changing these models. Functionalization is one manner of restricting the space of the solutions allowed to address ill-posedness, but many times, is not adequate. Therefore, additional constraints may need to be applied to restrict the solution space. There are many manners of performing regularization, ranging from those based upon "energy" minimization approaches to those based upon Bayesian decision analysis. A solid mathematical basis has been developed for unifying various regularization approaches and understanding under what conditions regularization is effective[25]-[29]. Effective regularization methods factor in uncertainties in observables (measurements), a priori and a posteriori knowledge of uncertainties in parameters to be adjusted, and robustness of adaptation. The a priori and a posteriori information are the best available information about model parameters before and after adaption is completed.

1.8. Scope of Work

Our target is to reduce the disagreement between actual plant data and core simulators' predictions of core attributes, however, at the current stage of project development, a virtual approach is utilized to develop insight into the proposed adaptive techniques. Chapter 2 discusses this approach in details and briefly discusses the core simulator we employed in the study (*e.g.* FORMOSA-B¹). The selected core simulator's parameterization is also presented. Chapter 3 is devoted to introducing the discretized version of the inverse theory which has been employed in our work. In chapter 4, some selected test cases associated with the virtual approach are investigated to assess the adaptive techniques. Chapter 5 presents our recommendations for further development in the area of adaptive core simulation.

1. Fuel Optimization for Reloads-Multiple Objectives by Simulated Annealing - BWR.

2. Virtual Approach

2.1. Description of the Virtual Approach

As mentioned in the introductory chapter, this thesis presents elementary work undertaken as a part of an exploratory project to develop adaptive simulation techniques which will enhance the agreement between measured and predicted core attributes, including core observables. Therefore, the main target in this work is to contrast the predictions of the adapted core simulator to actual plant data, in an effort to assess and validate the proposed techniques. However, since the project is still in its exploratory stages, a virtual approach will be adopted for assessing the fidelity and robustness of the techniques. In this approach, the actual plant data will be produced by an existing version of a core simulator, that will be referred to as a virtual core, denoted by VC. Since the plant data consists of the readings of incore detectors (*i.e.* LPRMs and TIPs signals), the virtual core will be used to simulate those detectors' responses, and in doing so the noise on those responses will also be simulated by perturbing their signals from their simulated values by sampling them from a Gaussian distribution of standard deviation of 0.04 of the average relative detectors' response which is a representative value of the actual instruments' noise signals. Since adaptive techniques are supposed to address and adjust for the different sources of prediction errors, an altered version of the same core simulator will be used after deliberately introducing two major sources of errors, specifically, in its modeling and in its input data. This version of the core simulator will be referred to as the design basis core simulator, denoted by DC. The size of the introduced errors in the DC will be chosen so as to create discrepancies between the predictions of the VC and DC for core reactivity and LPRM detectors' signals RMS errors of the same magnitude as

the actual discrepancies found between real plant data and existing core simulators' predictions. A representative value for the core reactivity prediction error is around $2\sigma = 1000$ pcm, and the RMS error for relative detectors' signals is about 6%. The FORMOSA-B core simulator[30]-[32] was utilized to both generate the values of the experimental observables and as the core simulator to be adapted.

2.2. Advantages of Virtual Approach Utilization

In contrast to utilizing operating power plant observables, the virtual core approach has several attractive properties in regard to developing an adaptive core simulator methodology, such as the following: 1) Knowing exactly the sources of errors in the method, input data and observables. 2) Providing a basis to study the effects of the parametrization of core simulator model on the fidelity and/or robustness of the adaptive simulator. 3) Having not to contend with the complexities of core simulator and pre-processor introduced methods' errors. 4) Being able to evaluate the prediction accuracies of non-observables (*i.e.* thermal margins) obtained from pre- and post-adaptation.

2.3. Core Parameterization

This section presents a brief description of the core models and input data which were perturbed and/or adapted in the virtual approach. In practice, as mentioned in the introductory chapter, the input data to be adapted will be first functionalized in terms of core parameters to render an over-determined problem. A detailed discussion of the parameterization selected in current work will be presented in this section as well.

2.3.1 Thermal-Hydraulics Core Parameterization (Simulation of Modeling Errors)

The first major source of prediction errors included in the virtual approach is the one due to modeling errors. The modeling of voids in a BWR core has a large impact on the prediction of different core attributes. Predictions of power distribution and reactivity are known to be very sensitive to the moderator void (density) distribution. That necessitates the utilization of a reasonably high fidelity void-quality correlation in order to predict core attributes to a reasonable degree. Based on that fact, the void-quality correlation was elected to be perturbed in the DC. The void-quality¹ relationship is given by the form first identified by Zuber-Findlay[33],

$$\alpha = x / \left(C_0 \left[x + \frac{\rho_g}{\rho_l} (1 - x) \right] + \frac{\rho_g V_{gj}}{G} \right), \quad (2-1)$$

where

$$V_{gj} = k_3 \left[\frac{(\rho_l - \rho_g)}{\rho_l^2} \sigma g \right]^{1/4}. \quad (2-2)$$

The DC utilized the Zuber-Findlay void-quality correlation in which two variables, the concentration parameter (C_0) and terminal velocity parameter (k_3), were assumed spatially independent throughout the core and given by their best known values,

$$C_0 = 1.13; \quad k_3 = 1.41 \quad (2-3)$$

Both variables were elected as input data to be adapted according to the relationship:

$$\tilde{C}_0 = f^{c_0} C_0; \quad \tilde{k}_3 = f^{k_3} k_3 \quad (2-4)$$

1. Refer to Moore's PhD thesis for more details[32].

where the factors f^{c_0} and f^{k_3} represent the selected thermal-hydraulics core parameters which are to be determined by the adaptive techniques, and \tilde{C}_0 and \tilde{k}_3 are the adapted void-quality constants utilized in the adapted design basis core simulator, denoted by AC, to calculate the void fraction. The virtual core utilized the Lellouche-Zolotar EPRI methodology[34] to determine C_0 and k_3 , which can be thought of as using spatially dependent C_0 and k_3 . The purpose of this difference in functionalizing the void-quality relationship between the VC and the DC is to investigate how well the adaptive technique will perform when the functionalization of the data is not consistent with reality, and how an adaptive technique can account separately for the combined sources of errors due to inconsistent modeling and input data errors.

2.3.2 Reactor Physics Core Parameterization

The second major source of errors included in the virtual approach is the one due to input data errors (*e.g.* thermal-hydraulics and reactor physics input data). The thermal-hydraulics data in the current study consists of only the C_0 and k_3 , coefficients of the Zuber-Findlay void-quality correlation. The reactor physics input data consists of all types of few-group homogenized fast and thermal microscopic cross-sections of all nuclides, included explicitly or implicitly in the microscopic depletion model of the utilized core simulator (*e.g.* FORMOSA-B). Table 2.1 presents the set (ζ) of all the fuel, burnable poison and pseudo isotopes considered in the core simulator model, and Table 2.2 presents the corresponding microscopic cross-section set (\aleph) selected for adjustment according to each nuclide's

Table 2.1: Isotopics treated in the core simulator model.

Treatment in Depletion Model	Element	Element-Isotope (Classification)
Explicit	Actinides	U-234 ⁽¹⁾ , U-235 ⁽⁴⁾ , U-236 ⁽⁴⁾ , Np-239 ⁽¹⁾ , U-238 ⁽³⁾ Pu-239 ⁽⁴⁾ , Pu-240 ⁽⁴⁾ , Pu-241 ⁽⁴⁾ , Pu-242 ⁽⁴⁾ , Am-243 ⁽⁴⁾
	Burnable poisons	Gd-154 ⁽²⁾ , Gd-155 ⁽²⁾ , Gd-156 ⁽²⁾ , Gd-157 ⁽²⁾ , Gd-158 ⁽²⁾
Implicit	Pseudo isotope	Represents background <i>macroscopic</i> cross-section ⁽⁵⁾ for elements not directly included in the depletion model.

(#) Nuclide Classification

Table 2.2: Selected set of adjusted microscopic cross-sections.

(#) Nuclide Classification	σ_{a1}	σ_{a2}	σ_{f1}	σ_{f2}	$\nu\sigma_{f1}$	$\nu\sigma_{f2}$	κ
(1) Transparent							
(2) Absorber	X	X					
(3) Fertile	X		X		X		X
(4) Fissile	X	X	X	X	X	X	X
(5) Pseudo	X	X	X	X	X	X	

(X) Denotes a cross-section type that is adjusted.

classification. The cross-section representation developed in FORMOSA-B[35] requires that a number of ‘cases’ be generated at the lattice physics level. Base micro and/or macroscopic cross-sections are obtained from a lattice physics unit assembly depletion at the nominal hot full power (HFP) average core conditions at different vapor void fractions. From these base depletions, branch cases are performed to capture the instantaneous effects of perturbing

different core conditions like fuel temperature, coolant void, and control rod insertion. This requires that different branch case calculations be made at various exposures within the set of the reference depletion exposures like fuel temperature decrease or increase, instantaneous void fraction correction, and control rod insertion at HFP. The data read from these branch cases along with the base depletions are used to model the local thermal-hydraulic feedback and transient fission product feedback effects. The cross-section is constructed as the summation of a reference and a set of correction terms given by:

$$\Sigma = \Sigma^{REF} + \Sigma^{CRH} + \Sigma^{TF} + \Sigma^{FP} + \Sigma^{CRD}, \quad (2-5)$$

where the reference term is the first term on the R.H.S. and is a function of fuel exposure, and instantaneous and history void fractions. The rest of the terms can be considered as correction terms, the first one is a function of control rod history, second one represents fuel temperature Doppler broadening effect, third one is due to fission products poisoning, and the last one represents the instantaneous control rod insertion effect. The reference and the correction terms are constructed using piece-wise cubic splines and quadratic fitting polynomials. A reference or correction term k of a cross-section type j for a nuclide n in a fuel color c is given by:

$$\Sigma^{n,j,k,c}(Bu) = \sum_{i=1}^I d_i^{n,j,k,c}(Bu) y_i(\bar{x}), \quad (2-6)$$

where \bar{x} is a state variable describing the dependence of the specific cross-section reference or correction term on different core conditions (*i.e.* fuel temperature, void fraction, etc.),

$\{d_i^{n,j,k,c}\}$ are the polynomial coefficients calculated based on the lattice physics data, and are

functionalized in terms of the fuel exposure, Bu , and $\{y_i\}$ are polynomial functions. The base or correction terms are adapted according to the relation:

$$\tilde{\Sigma}^{n,j,k,c}(Bu) = \sum_{i=1}^I f_i^{n,j,k,c}(Bu) d_i^{n,j,k,c}(Bu) y_i(\bar{x}) \quad (2-7)$$

where the $f_i^{n,j,k,c}$ factors are functionalized in terms of fuel exposure according to the following relation:

$$f_i^{n,j,k,c}(Bu) = f_{i,1}^{n,j,k,c} + (1 - f_{i,2}^{n,j,k,c}) \frac{Bu}{\tilde{Bu}} \quad (2-8)$$

with the factors $\{f_{i,1}^{n,j,k,c}, f_{i,2}^{n,j,k,c}\}$ representing the reactor physics core parameters which are to be determined by the adaptive techniques, and \tilde{Bu} is a scaling factor with exposure units.

2.4. Simulation of Input Data Errors

The direct approach to simulate input data errors would be one in which each input data from the set studied (*e.g.* C_0 , k_3 and the lattice physics few-group homogenized cross-sections library) is randomly selected from a normalized Gaussian distribution whose standard deviation corresponds to the relative uncertainty for that specific input data. One can then assume that the perturbed values are our current best knowledge of these data.

The uncertainty information is not directly available though, and to obtain it, one would need to propagate the uncertainty information starting from an energy point-wise or resonance parameters presentation like ENDF/B to a few group, spatially homogenized

presentation provided by most lattice physics codes. This is not a trivial task to do and requires substantial calculational efforts. For that reason and for the sake of an exploratory investigation, a cruder approach will be utilized. In this approach, the input data are considered to be fully characterized by the selected core parameters¹ (e.g. f^{c_0} , f^{k_3} , and $\{f_{i,1}^{n,j,k,c}, f_{i,2}^{n,j,k,c}\}$). To simulate input data errors in this cruder approach, each of the core parameters will be randomly selected from a normalized Gaussian distribution whose standard deviation is assumed now to be the same for all core parameters. A constant standard deviation (1%) is selected, so as to give rise to discrepancies between the predictions (LPRMs readings and core reactivity) of the VC and DC which are representative of the actual magnitude of such discrepancies found between real plant data and existing core simulators. After perturbing the core parameters in this fashion, the original input data can be represented by:

$$\hat{C}_0 = \hat{f}^{c_0} C_0; \quad \hat{k}_3 = \hat{f}^{k_3} k_3; \quad \hat{d}_i^{n,j,k,c} = \left(\hat{f}_{i,1}^{n,j,k,c} + (1 - \hat{f}_{i,2}^{n,j,k,c}) \frac{Bu}{\bar{B}u} \right) d_i^{n,j,k,c} \quad (2-9)$$

where now the perturbed core parameters (e.g. \hat{f}^{c_0} , \hat{f}^{k_3} , and $\{\hat{f}_{i,1}^{n,j,k,c}, \hat{f}_{i,2}^{n,j,k,c}\}$) will be assumed to constitute our best knowledge (e.g. the a priori information) about the input data to simulate input data errors in the virtual approach.

Note that each of the reference and corrections terms are functionalized in terms of the void fraction (through $y_i(\bar{x})$), so when one is adapting the void-quality parameters and the polynomial coefficients as well, one is explicitly correcting separately for the void-quality

1. Note that the unperturbed values for the selected core parameters are all equal to 1.0.

modeling error and the input data errors (to a first-order approximation). Consider a small perturbation in all the core parameters, the resulting perturbation in the cross-section is given by,

$$\Sigma^{n,j,k,c} + \Delta\Sigma^{n,j,k,c} = \sum_{i=1}^I (f_i^{n,j,k,c} + \Delta f_i^{n,j,k,c}) d_i^{n,j,k,c} (y_i(\bar{x}) + \Delta y_i(\bar{x}))$$

where to a first order approximation, $\Delta y_i(\bar{x})$ is given by,

$$\Delta y_i(\bar{x}) = \frac{\partial}{\partial f^{c_0}} y_i(\bar{x}) \Delta f^{c_0} + \frac{\partial}{\partial f^{k_3}} y_i(\bar{x}) \Delta f^{k_3},$$

and hence,

$$\begin{aligned} \Delta\Sigma^{n,j,k,c} &= f_i^{n,j,k,c} d_i^{n,j,k,c} \frac{\partial}{\partial f^{c_0}} y_i(\bar{x}) \Delta f^{c_0} \\ &\quad + f_i^{n,j,k,c} d_i^{n,j,k,c} \frac{\partial}{\partial f^{k_3}} y_i(\bar{x}) \Delta f^{k_3} \\ &\quad + \sum_{i=1}^I y_i(\bar{x}) d_i^{n,j,k,c} \Delta f_i^{n,j,k,c} \end{aligned}$$

However, if one is not adapting the void-quality correlation, the adjusted reactor physics core parameters $\{f_i^{n,j,k,c}\}$ will be accounting both for input data and modeling errors as well, but only for those specific core conditions at which the adaption was completed (*e.g.* certain core average void fraction). That could lead to a less robust adaption when trying to predict core behaviour at different core conditions. This issue will be investigated in the study to show how powerful the adaption can be utilized to separately adjust for the different sources of prediction errors and give insight to situations when adaption is performed on the wrong input parameters.

To simplify the adaption, dependencies of the reactor physics core parameters $\{f_i^{n,j,k,c}\}$ will be restricted to nuclides (n) and reactions types (j) with dependencies on correction terms (k), fuel colors (c) and fitting polynomials (i) dropped. In reality, correction terms are expected to be dependent upon branch cases and fuel color, since the unit lattice flux energy and spatial shapes are dependent upon these attributes. Hence, the few-group homogenized cross-sections errors are also dependent on different branch cases and fuel colors. As this project moves forward, more sophistication will be introduced. Even with this simplification, a total of 108 core parameters were free to adapt.

3. Discrete Inverse Theory

3.1. Objective

The applications of the inverse theory are diverse and include many areas of science; however, the emphasis in this work will mainly be on core physics problems. Most of the introduced nomenclature, notations and examples are selected specifically to serve our application. Minor modifications are required to generalize the methods and discussion to other areas of interest. The subject of the generalized inverse theory is very mathematical in nature and most of the ideas need extensive rigor and mathematical abstraction to be comprehensively and concisely presented. The mathematical tools necessary for our work will be presented; however, the discussion will not be highly mathematical and is not intended to be neither comprehensive nor complete. The intent is to present the more intuitive ideas behind the utilization of these tools rather than the more abstract mathematical rigor. We choose to do this for three reasons: 1) The more extensive and rigorous treatment of the subject is already well established in the literature and stands on a very firm basis[25]-[26], so it would be redundant to reproduce these mathematical results in this work even in part. 2) We believe in a more realistic illustration of the abstract mathematical ideas, and that heavy abstraction serves to generalize rather than to develop our understanding about certain phenomena. Hopes for solving more complicated problems by utilizing the abstract and more complicated version of the theory are rarely encountered in practice. 3) Our work is intended primarily for engineers rather than for mathematicians. For these reasons, the concepts are emphasized more than the technicalities in order to avoid confusion. Narrative discussions and simplified examples are stressed rather than the more rigorous treatment of the subject.

However, to avoid a speculative type discussion, an extensive bibliography will be referenced to support the discussion whenever necessary.

The discussion will be confined to the discrete linear inverse theory. This implies that, in order to apply the theory, we will need to linearize the core simulator model and employ an iterative strategy to search for the optimum core parameters' values. Almost every problem in discrete inverse theory can be recast into an optimization problem, where a function must be minimized subject to various constraints. Optimization techniques for discrete problems can best be described by vector space methods since the whole theory can then be derived from a few simple, intuitive and geometric relations. A large number of problems can be analyzed utilizing those simple relations. The texts by Luenberger[30] and Dorny[24] present comprehensive and insightful approaches to optimization methods using vector space methods.

3.2. Definitions

In this section an informal survey of some of the essential definitions, within the context of our application, is introduced[21],[36].

3.2.1 Parameter Space

The parameter space is defined as the vector space whose elements represent the set of core parameters we are trying to estimate. Let n be the number of such parameters, and $\Delta\bar{p}$ a vector of dimension n which lies in the parameters space R^n ($\Delta\bar{p} \in R^n$) and denotes the core parameters.

3.2.2 Data (Observables) Space

The data space is defined as the vector space whose elements are the values of the core observables. Let m be the number of such observables, and let $\Delta\bar{d}^m$ and $\Delta\bar{d}^c$ be vectors of dimension m which lie in the data space R^m ($\Delta\bar{d}^m, \Delta\bar{d}^c \in R^m$) and denote the measured and predicted (calculated) observables, respectively¹.

3.2.3 Linear Transformation

A function Ψ that associates with every point $\Delta\bar{p} \in R^n$ in the parameters' space a point $\Delta\bar{d}^c \in R^m$ in the data space is said to be linear if it satisfies the following condition,

$$\Psi(\alpha_1 \Delta\bar{p}_1 + \alpha_2 \Delta\bar{p}_2) = \alpha_1 \Psi(\Delta\bar{p}_1) + \alpha_2 \Psi(\Delta\bar{p}_2) \quad \text{for all scalars } \alpha_1 \text{ and } \alpha_2 \quad (3-10)$$

where $\Delta\bar{p}_1, \Delta\bar{p}_2 \in R^n$. The action of a linear function is referred to as a linear transformation which can be characterized by a matrix operator $\bar{\bar{A}}$. One can visualize the operation of such a transformation from different view points. Meyer[37] presents one such rigorous and insightful discussion of the subject. Linear transformation is the process in which each point $\Delta\bar{p} \in R^n$ in the parameters space is mapped to a unique point $\Delta\bar{d}^c \in R^m$ in the observables space, this unique correspondence determined by the matrix $\bar{\bar{A}}$, where $\bar{\bar{A}} \in R^{m \times n}$ and can be described by,

1. The Δ notations are enforced here to avoid introducing extra notations later in the discussion since the linearization of the core simulator model will require the utilization of these notations. Δ notation denotes the difference between the variable of interest (*e.g.* core parameters or observables) and some reference value.

$$\Delta \bar{d}^c = \bar{\bar{A}} \Delta \bar{p}. \quad (3-11)$$

3.2.4 SVD Decomposition

To gain more insight into the anatomy of such a transformation, the SVD decomposition of the matrix $\bar{\bar{A}}$ is introduced[38]-[40]. Any matrix $\bar{\bar{A}} \in R^{m \times n}$ has an orthogonal decomposition such that,

$$\bar{\bar{A}} = \bar{\bar{U}} \bar{\bar{S}} \bar{\bar{V}}^T, \quad (3-12)$$

where $\bar{\bar{U}}$ and $\bar{\bar{V}}$ are orthogonal matrices (their columns constitute orthonormal bases for the spaces R^m and R^n , respectively). The columns of $\bar{\bar{U}}$ and $\bar{\bar{V}}$ are called the left and right singular vectors of the matrix $\bar{\bar{A}}$. $\bar{\bar{S}}$ is a diagonal matrix containing the singular values of the matrix $\bar{\bar{A}}$. These matrices are given by,

$$\bar{\bar{U}}^{m \times m} = [\bar{u}_1 \ \bar{u}_2 \ \dots \ \bar{u}_m], \quad \bar{\bar{V}}^{n \times n} = [\bar{v}_1 \ \bar{v}_2 \ \dots \ \bar{v}_n],$$

$$\bar{\bar{S}}^{m \times n} = \begin{bmatrix} \sigma_1 & & & & & \\ & \sigma_2 & & & & \\ & & \ddots & & & \\ & & & \sigma_r & & \\ & & & & 0 & \\ & & & & & \ddots \\ & & & & & & 0 \dots 0 \end{bmatrix},$$

where

$$\bar{u}_i^T \bar{u}_j = \delta_{ij} \quad \text{for} \quad 1 \leq i, j \leq m,$$

$$\bar{v}_i^T \bar{v}_j = \delta_{ij} \quad \text{for} \quad 1 \leq i, j \leq n,$$

and δ_{ij} is the Kronecker delta function. The right and left singular vectors satisfy the following relations:

$$\bar{\bar{A}} \bar{v}_i = \sigma_i \bar{u}_i \text{ for } 1 \leq i \leq r,$$

$$\bar{\bar{A}} \bar{v}_i = \bar{0} \text{ for } r < i \leq n,$$

and

$$\bar{\bar{A}}^T \bar{u}_i = \sigma_i \bar{v}_i \text{ for } 1 \leq i \leq r,$$

$$\bar{\bar{A}}^T \bar{u}_i = \bar{0} \text{ for } r < i \leq m.$$

Now denote the two basis defined by the columns of $\bar{\bar{U}}$ and $\bar{\bar{V}}$ by $B_{\bar{\bar{U}}}$ and $B_{\bar{\bar{V}}}$, respectively¹.

One can re-write Eq. (3-11) as,

$$\bar{\bar{A}} \Delta \bar{p} = \bar{\bar{U}} \bar{\bar{S}} \bar{\bar{V}}^T \Delta \bar{p} = \sum_{i=1}^r (\sigma_i \bar{v}_i^T \Delta \bar{p}) \bar{u}_i = \sum_{i=1}^r (\sigma_i \Delta \dot{\bar{p}}_i) \bar{u}_i = \sum_{i=1}^r \Delta \dot{\bar{d}}_i^c \bar{u}_i = \Delta \bar{d}^c. \quad (3-13)$$

Note the following:

1. Summation extends from $i = 1$ to $i = r$, since only the first r singular values are non-zero, where r is equal to the rank of matrix $\bar{\bar{A}}$.
2. $\Delta \dot{\bar{p}}_i = \bar{v}_i^T \Delta \bar{p}$ is the component of $\Delta \bar{p}$ along the direction of the right singular vector \bar{v}_i .

1. Note that the different orthogonal directions defined by the bases $B_{\bar{\bar{V}}}$ and $B_{\bar{\bar{U}}}$ are not unique in general. For a general $m \times n$ matrix, the $\{\bar{u}_i\}$ and $\{\bar{v}_i\}$ vectors associated with any subset of singular values which are distinct are necessarily unique. If however, some of the singular values are equal, then the associated right and left singular vectors can be chosen arbitrarily, since the components of either the parameters or the observables along these directions are amplified by the same amount.

3. $\Delta \dot{\bar{d}}_i^c$ is the component of $\Delta \bar{d}^c$ along the direction of the left singular vector \bar{u}_i .

3.2.5 Anatomy of Linear Transformation

The action of transformation can be interpreted in the following way:

1. The vector $\Delta \bar{p}$ (given initially with respect to the standard basis in R^n) is resolved along each of the right singular vectors \bar{v}_i of the basis $B_{\bar{v}}$.
2. Each of the components $\Delta \dot{\bar{p}}_i$ in the new basis is multiplied by the corresponding singular value σ_i .
3. The result is the component of the mapped vector $\bar{\bar{A}}\Delta \bar{p}$ along the direction of each of the left singular vectors \bar{u}_i of the basis $B_{\bar{u}}$.
4. The mapped vector $\bar{\bar{A}}\Delta \bar{p}$ is presented back in terms of the standard basis in R^m .

Note: If $r < \min(n, m)$ then:

1. For a given $\Delta \bar{p}$, the last $n - m$ components of $\Delta \bar{p}$ with respect to $B_{\bar{v}}$ will not be mapped to R^m (e.g. lost due to the transformation, and are not reflected in the vector $\Delta \bar{d}^c$). In a loose sense, the vector $\Delta \bar{d}^c$ does not have any information about the last $n - m$ components of the vector $\Delta \bar{p}$.
2. For a given $\Delta \bar{d}^c$, the last $m - n$ components with respect to $B_{\bar{u}}$ cannot be produced by the mapping $\bar{\bar{A}}$ and have to be equal to zero for the system of equations given by Eq. (3-11) to

be consistent. However, if these components are not zero for the given $\Delta \vec{d}^c$ (e.g. measured observables), they cannot be explained by the linear transformation $\bar{\bar{A}}$ and must have originated from other sources (*i.e.* noise in the measured data or modeling errors).

3.2.6 Reverse Transformation

If we take the transpose of $\bar{\bar{A}}$, denoted $\bar{\bar{A}}^T$, and operate on a vector $\Delta \vec{d}^m$ which belongs to the data space, we obtain using the SVD

$$\bar{\bar{A}}^T \Delta \vec{d}^m = \sum_{i=1}^r (\sigma_i \bar{u}_i^T \Delta \vec{d}^m) \bar{v}_i, \quad (3-14)$$

which can be interpreted in the reverse manner then noted above, corresponding to mapping from R^m to R^n .

Figure 3.1 illustrates the action of the operator $\bar{\bar{A}}$ and $\bar{\bar{A}}^T$, showing how information is either mapped or lost due to transformation between the parameters and data spaces. One can observe the range, R and the null space, N of the operator $\bar{\bar{A}}$ and $\bar{\bar{A}}^T$. It is also evident that,

$$R(\bar{\bar{A}}) \perp N(\bar{\bar{A}}^T) \quad \text{and} \quad R(\bar{\bar{A}}^T) \perp N(\bar{\bar{A}}), \quad (3-15)$$

since $\bar{\bar{U}}$ and $\bar{\bar{V}}$ are orthogonal matrices (columns of each matrix are orthogonal to one another). Those four subspaces introduced in Eq. (3-15) are referred to as the four fundamental subspaces associated with the matrix $\bar{\bar{A}}$.

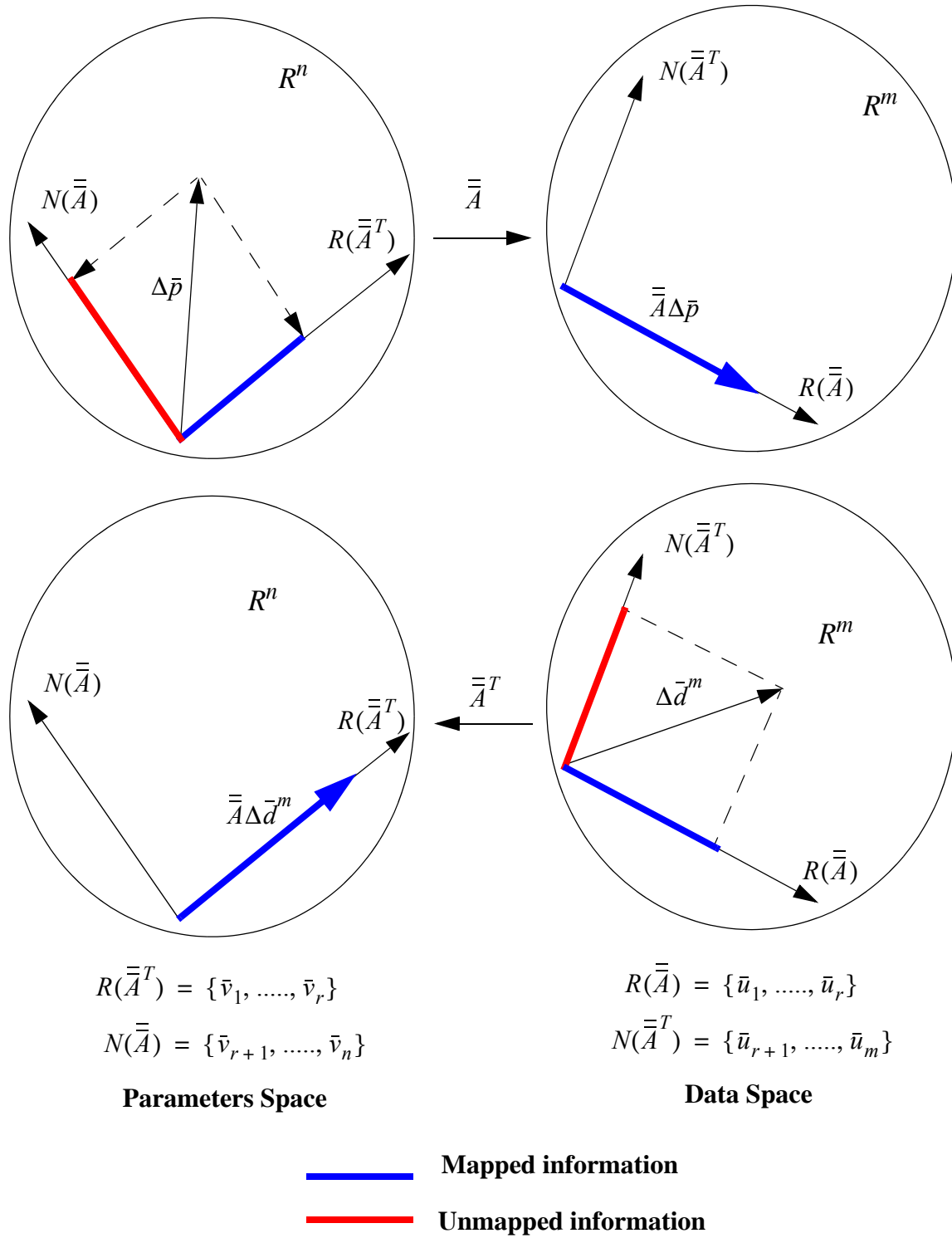


Figure 3.1: Mapping Information between Parameters and Data Spaces.

3.2.7 Inverse Transformation

One is also interested in the inverse transformation, that being how can one calculate $\Delta\bar{p}$ in the parameters space for a given $\Delta\bar{d}^m$ that lies in the data space. Referring to Eq. (3-13), one can reverse the action of the transformation by simply dividing the components of $\Delta\bar{d}^m$ along the directions of the left singular vectors $\{\bar{u}_i\}$ by the corresponding singular values $\{\sigma_i\}$. In doing so, one would not be able to map back those components of $\Delta\bar{d}^m$ which lie in $N(\bar{A}^T)$ since they are not produced by the forward transformation \bar{A} . In the least-squares solution, one ignores those components and only maps back to the parameters space those components which lie in the range of the operator, $R(\bar{A})$. One also would not be able to calculate the components of $\Delta\bar{p}$ which lie in $N(\bar{A})$ since they are lost in the forward transformation and no information is reflected about them in the observables. The solution $\Delta\bar{p}$ can then be written as

$$\Delta\bar{p} = \sum_{i=1}^r \left(\frac{1}{\sigma_i} \Delta\dot{\bar{d}}_i^m \right) \bar{v}_i + \sum_{i=r+1}^n \Delta\dot{\bar{p}}_i \bar{v}_i, \quad (3-16)$$

where $\{\Delta\dot{\bar{p}}_i\}_{i=r+1,n}$ are selected arbitrarily and $\{\Delta\dot{\bar{d}}_i^m\}$ are the components of $\Delta\bar{d}^m$ along the directions of the left singular vectors $\{\bar{u}_i\}$. In practice, one does not need to calculate the matrices \bar{U} and \bar{V} to obtain the least-squares solution; however, one utilizes the normal equations formulation[41] which can be shown to be equivalent to the approach suggested in

(7). If $\bar{\bar{A}}$ has a full column rank $r = n$ and $m > n$, this situation is referred to as an overdetermined problem whose least-squares solution is given by

$$\Delta \bar{p} = (\bar{\bar{A}}^T \bar{\bar{A}})^{-1} \bar{\bar{A}}^T \Delta \bar{d}^m. \quad (3-17)$$

The SVD decomposition of the matrix $\bar{\bar{A}}^T \bar{\bar{A}}$ is given by

$$\bar{\bar{A}}^T \bar{\bar{A}} = \bar{\bar{V}} \bar{\bar{S}}^* \bar{\bar{V}},$$

where

$$\bar{\bar{S}}^{*n \times n} = \begin{bmatrix} \sigma_1^2 & & & \\ & \sigma_2^2 & & \\ & & \ddots & \\ & & & \ddots \\ & & & & \sigma_n^2 \end{bmatrix}.$$

If $r < \min(n, m)$, the solution is not unique and the matrix $\bar{\bar{A}}^T \bar{\bar{A}}$ is singular, (e.g. has $n - r$ zero singular values).

3.2.8 Ill-posedness and Ill-conditioning

An inverse problem based on least-squares criterion has to satisfy Hadamard's three conditions to be well-posed. These conditions can abstractly be described as follows: For every $\varepsilon > 0$ such as $\|\Delta \bar{d}_1^m - \Delta \bar{d}^m\| < \varepsilon$, there exists a $\delta > 0$ such as $\|\Delta \bar{p}_1 - \Delta \bar{p}\| < \delta$. This implies that the solution $\Delta \bar{p}$ exists for every $\Delta \bar{d}^m$, is unique, and small perturbations in the measured observables result in small perturbations in the solution. If the least-squares problem does not satisfy these conditions, it is referred to as an ill-posed problem. The ill-conditioning of a problem, however, is related to the relative magnitudes of δ and ε . In a qualitative sense,

if $\delta \gg \varepsilon$ the problem is said to be ill-conditioned. For the overdetermined least-squares problem in Eq. (3-17), ill-conditioning can quantitatively be measured by a condition number, which is given by,

$$K = \frac{\sigma_{max}^2}{\sigma_{min}^2}, \quad (3-18)$$

where K is the condition number of the associated least-squares matrix, $\bar{\bar{A}}^T \bar{\bar{A}}$.

According to this, a least-squares problem is well-posed whenever all singular values are strictly greater than zero (the matrix $\bar{\bar{A}}^T \bar{\bar{A}}$ is non-singular and its rank is equal to n). Mathematically, the distinction between ill-posedness and ill-conditioning is very clear. An ill-conditioned least-squares problem, with a very large condition number K , can still be considered well-posed as long as it satisfies Hadamard's continuity conditions. However, from a computational point of view the distinction is not as clear-cut. A matrix which is mathematically non-singular, can be numerically near singular due to the finite number of significant digits used in a computer (the inverse of the matrix $\bar{\bar{A}}^T \bar{\bar{A}}$ cannot be calculated to an acceptable degree of precision). So a numerically near singular matrix corresponding to an ill-conditioned, well-posed problem is indistinguishable from a mathematically singular one corresponding to an ill-posed problem.

Some of the factors which result in a near singular matrix include the relative magnitudes of the singular values, and the magnitude of the noise in the measured observables. Refer to Eq. (3-16) and consider the components $\{\Delta \dot{\bar{d}}_i^m\}$ of the measured observables with respect to $B_{\bar{U}}$. In some situations some of these components are very small

compared to the noise level, or the singular values associated with these components are too small, leading to an unreliable and a random (dominated and mainly determined by the random noise) estimate of $\Delta\bar{p}$. That leads to an effective reduction of the rank r of the matrix \bar{A} (e.g. a near-singular matrix).

In these situations, the distinction between the four fundamental subspaces associated with the matrix becomes less clear. The terms “*near*” null space and “*effective*” range of a matrix will be utilized in the discussion to denote such situations¹[24]. As an example, consider the near null-space of a matrix, that will consist of all the right singular vectors whose corresponding singular values are very small. The effective range of a matrix will include all the left singular vectors whose corresponding singular values are considerably large.

In a loose sense, the rank of a matrix presents how much ‘content’ or ‘pieces of information’ a matrix can send (map) between two spaces[37] (i.e. in R^3 , a plane has more content in it than a line). Therefore, the linear transformations represented by the matrix \bar{A} and \bar{A}^T can send uniquely r pieces of information (e.g. components) back and forth between the parameters and data space. An overdetermined, ill-conditioned least-squares problem can effectively map less ‘content’ or ‘pieces of information’ than does a well-conditioned problem. Note that each piece of information sent from the parameters space is an amplified (due to the singular values) linear combination of all the parameters, and this piece of information appears in the data space as a linear combination of all the observables.

1. That distinction is merely for illustration purposes and will not explicitly be utilized in the work.

3.2.9 Forward Problem

In the forward problem, one is seeking information about core observables. They are directly obtained by mapping information about the core parameters from the parameters to data space. In this case, the nonlinear core model is employed.

3.2.10 Inverse Problem

In the inverse problem, one is seeking information about model parameters. Direct mapping of information from the data to parameters space usually poses a problem and results in an unreliable estimate of core parameters, which will be described in detail later. One of the goals of inverse theory is to determine how this information about model parameters can be inferred from the data without destroying the quality of the estimated parameters. In this case, we employ an iterative inversion of the linearized core model.

3.2.11 Measure of Distance

It is important to have a certain measure of the “difference” between two points (*e.g.* a quantitative measure of how far two points are from each other) in the parameters or data space. That difference will define our notion of distance and will generally be based on a certain criterion we select. For example, the crow flight distance represents the common intuition about the distance between two points in 3-D geometry[37]. It is referred to as the Euclidean measure of the distance and can be extended to higher dimensional spaces where it is given by:

$$\text{Euclidean distance between } \Delta \bar{d}^m \text{ and } \Delta \bar{d}^c \text{ in } R^m = \left[\sum_{j=1}^m (\Delta \bar{d}_j^m - \Delta \bar{d}_j^c)^2 \right]^{1/2}, \quad (3-19)$$

where the j index runs over the different components of the vectors $\Delta \vec{d}^m$ and $\Delta \vec{d}^c$. However, this is not necessarily the only way to measure the distance. For example, measuring distance on a grid of city blocks on one-way streets, one would rather measure the distance in this case on the directed grid rather than the crow flight distance. Another example, one can think of a more generalized sum of the type given by Eq. (3-19), in which different weights are assigned to different components to reflect different degrees of uncertainties in the measurements or the calculations. The criterion we choose to define the distance will alter our qualitative and/or quantitative measure of the distance between two points in the vector space of interest (*i.e.* far, close, etc.)

Norms represent the mathematical abstraction utilized to measure the distance between any two points in the vector space. Norms satisfy certain relationships, which are in accordance with our intuition about the notion of Euclidean distance; however, the concept of distance is generalized in a more rigorous fashion. A vector norm is a function $\|\cdot\|$ which maps a vector space of dimension m , R^m into R^1 (the real line), and satisfies the following relations[37]:

$$\begin{aligned} \|\Delta \vec{d}\| &\geq 0 \quad \text{and} \quad \|\Delta \vec{d}\| = 0 \Leftrightarrow \Delta \vec{d} = 0 \\ \|\alpha \Delta \vec{d}\| &= |\alpha| \|\Delta \vec{d}\| \quad \text{for all scalars } \alpha \\ \|\Delta \vec{d}_1 + \Delta \vec{d}_2\| &\leq \|\Delta \vec{d}_1\| + \|\Delta \vec{d}_2\|. \end{aligned} \tag{3-20}$$

where $\Delta \vec{d}, \Delta \vec{d}_1, \Delta \vec{d}_2 \in R^m$.

An important family of norms is referred to as the p -Norms. A general member of this family is given by,

$$\|\Delta \bar{d}\|_p = \left(\sum_{j=1}^m |\Delta \bar{d}_j|^p \right)^{\frac{1}{p}}. \quad (3-21)$$

The three most important members of this family are given by,

$$\begin{aligned} \|\Delta \bar{d}\|_1 &= \sum_{j=1}^m |\Delta \bar{d}_j|; & \|\Delta \bar{d}\|_2 &= \sqrt{\sum_{j=1}^m |\Delta \bar{d}_j|^2} \\ \|\Delta \bar{d}\|_\infty &= \lim_{p \rightarrow \infty} \|\Delta \bar{d}\|_p = \max_j |\Delta \bar{d}_j| \end{aligned}$$

Inner products are another way of producing norms. It can be proved mathematically that every general inner product $\langle *, * \rangle$ in an inner product space¹ defines a vector norm $\|*\|$ on that space according to the relation[30],[37],

$$\|\Delta \bar{d}\| = \sqrt{\langle \Delta \bar{d}, \Delta \bar{d} \rangle}.$$

The definition of inner product will be deferred till the notion of best approximation is introduced.

3.2.12 Best Approximation

As mentioned in a previous section, when the rank r of the matrix $\bar{\bar{A}}$ is less than the dimension m of the data space, the observables $\Delta \bar{d}^m$ can have components only along the range of the operator $\bar{\bar{A}}$. That is necessary for the system of equations $\bar{\bar{A}}\Delta \bar{p} = \Delta \bar{d}^m$ to be consistent. However, these observables are usually measured quantities and are utilized in practice to infer information about core parameters. One then needs a method to remove this

1. Any finite dimensional space is an inner product space, see [30].

extra unexplained information (components) from the observables. The notion of best approximation denotes one such method. Refer to Figure 3.2, assume that the point $\Delta \bar{d}^m \in R^m$ is a measured quantity, and the subspace $R(\bar{\bar{A}})$ represents our theory (our best possible interpretation of the relationship between the core observables and model parameters). In practice, the measurements do not match the theory. An important problem that arises is to find the closest point to the measurements that is consistent with the model. That point will denote the best prediction of core observables that can be obtained utilizing our theory. The solution to that problem will depend on our definition of closeness (*e.g.* the norm utilized to measure the distance), and generally different norms will result in different points on the model. Figure 3.2 shows the neighbourhood of the point $\Delta \bar{d}^m$ described by a circle $O(r_p)$ of

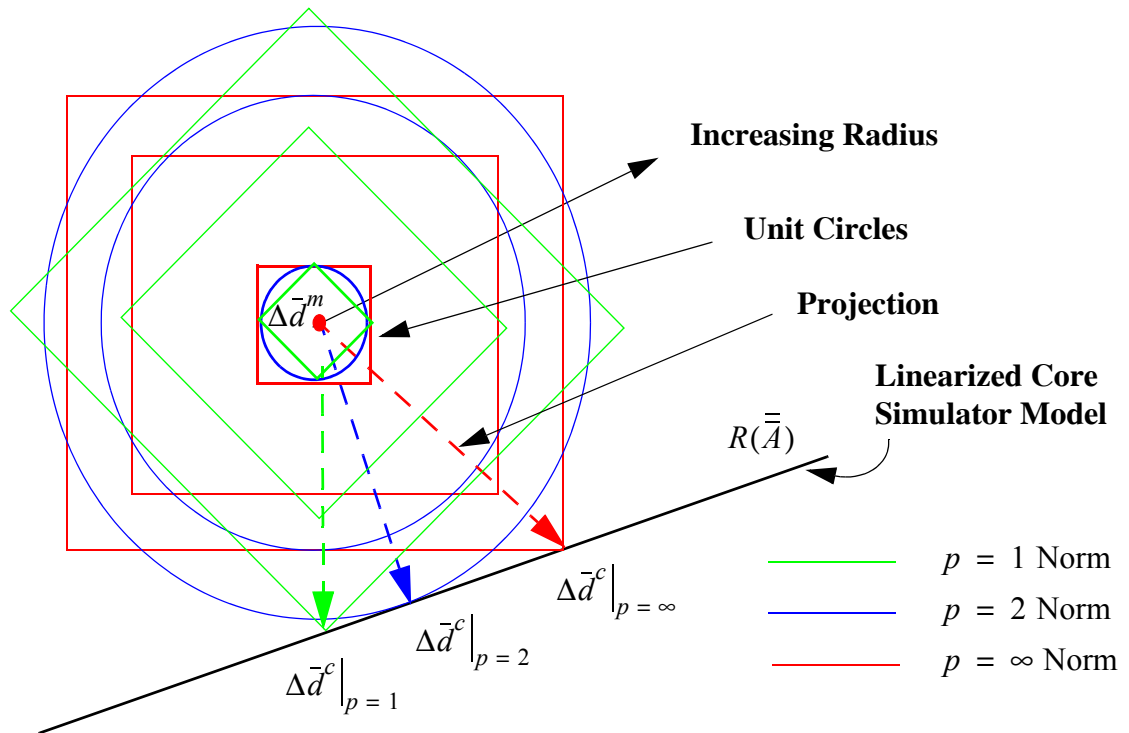


Figure 3.2: Notion of Best Approximation.

radius r_p ($O(r_p) = \{\Delta\bar{d} \in R^m \mid \|\Delta\bar{d}^m - \Delta\bar{d}\|_p \leq r_p\}$). Different norms give rise to different shaped circles. To get the closest point, consistent with the model, to the observables, the radius r_p of the circle $O(r_p)$ is increased gradually till it intersects the model, $R(\bar{\bar{A}})$. The first point at which intersection occurs will represent the closest point to the measurements that satisfies the model. The difference $\Delta\bar{d}^m - \Delta\bar{d}^c$ represents the prediction errors made by the theory and can quantitatively be measured by any general norm. Note that the solution (*e.g.* location of the closest point) is not unique in general, and to obtain it using a general norm (*i.e.* 1-Norm) is not an easy problem, since it does not involve a simple functional form to be minimized by ordinary calculus. To overcome these difficulties, the inner product-based norms are introduced.

3.2.13 Inner Product and Orthogonality

Let $\Delta\bar{d}_1, \Delta\bar{d}_2 \in R^m$, the standard inner product on R^m is defined by:

$$\langle \Delta\bar{d}_1, \Delta\bar{d}_2 \rangle = \Delta\bar{d}_1^T \Delta\bar{d}_2 = \sum_{j=1}^m \Delta\bar{d}_{1j} \Delta\bar{d}_{2j}, \quad (3-22)$$

where $\{\Delta\bar{d}_{1j}\}$ and $\{\Delta\bar{d}_{2j}\}$ are the components of $\Delta\bar{d}_1$ and $\Delta\bar{d}_2$ with respect to the standard basis in R^m . For the sake of our purposes, let us define the following specific form of inner product:

$$\langle \Delta\bar{d}_1, \Delta\bar{d}_2 \rangle_{\bar{\bar{C}}} = \Delta\bar{d}_1^T \bar{\bar{C}} \Delta\bar{d}_2, \quad (3-23)$$

where $\bar{\bar{C}}$ is a symmetric positive definite matrix. $\bar{\bar{C}}$ can be made diagonal by an orthogonal transformation[37] which can be written as,

$$\bar{\bar{C}} = \bar{\bar{W}}\bar{\bar{\Lambda}}\bar{\bar{W}}^T, \quad (3-24)$$

where $\bar{\bar{W}}$ and $\bar{\bar{\Lambda}}$ are orthogonal and diagonal matrices respectively. One can re-write the inner product in Eq. (3-23) as,

$$\begin{aligned} \langle \Delta \bar{d}_1, \Delta \bar{d}_2 \rangle_{\bar{\bar{C}}} &= \Delta \bar{d}_1^T \bar{\bar{C}} \Delta \bar{d}_2 = \Delta \bar{d}_1^T \bar{\bar{W}} \bar{\bar{\Lambda}} \bar{\bar{W}}^T \Delta \bar{d}_2 \\ &= (\bar{\bar{W}}^T \Delta \bar{d}_1)^T \bar{\bar{\Lambda}} (\bar{\bar{W}}^T \Delta \bar{d}_2) = \sum_{j=1}^m \Lambda_j \Delta \dot{\bar{d}}_{1j} \Delta \dot{\bar{d}}_{2j} \end{aligned} \quad (3-25)$$

where now, $\Delta \dot{\bar{d}}_{1j}$ and $\Delta \dot{\bar{d}}_{2j}$ are the components of $\Delta \bar{d}_1$ and $\Delta \bar{d}_2$ with respect to the basis described by the columns of $\bar{\bar{W}}$, and the product of each respective component is weighed by the j th diagonal element Λ_j of the matrix $\bar{\bar{\Lambda}}$. Two vectors $\Delta \bar{d}_1$ and $\Delta \bar{d}_2$ are said to be orthogonal if they satisfy the following criterion,

$$\langle \Delta \bar{d}_1, \Delta \bar{d}_2 \rangle_{\bar{\bar{C}}} = 0. \quad (3-26)$$

Note that according to this definition, the notion of orthogonality will depend on the form of the inner product selected in the application.

One can now define an inner product-based norm in the following fashion,

$$\|\Delta \bar{d}\|_{\bar{\bar{C}}} = \sqrt{\langle \Delta \bar{d}, \Delta \bar{d} \rangle_{\bar{\bar{C}}}}. \quad (3-27)$$

The subscript on the norm denotes that it is produced from an inner product norm utilizing a symmetric positive definite matrix $\bar{\bar{C}}$. One can show that this norm satisfies the norm

requirements defined in Eq. (3-20). In addition, this norm has two important properties. First, it provides a mathematical criterion that can be utilized effectively to find the “closest point” on the model to our observables (*i.e.* elements from ordinary calculus can be utilized to find the solution). Second, the mathematical criterion results in a unique solution and is of the form,

$$\langle \Delta \vec{d}^m - \Delta \vec{d}^c, R(\bar{\bar{A}}) \rangle_{\bar{\bar{C}}} = 0. \quad (3-28)$$

Eq. (3-28) may be described as follows: Find the point $\Delta \vec{d}^c$ on the range of the operator $\bar{\bar{A}}$ such that the residual vector $\Delta \vec{d}^m - \Delta \vec{d}^c$ (*e.g.* components of the observables that cannot be explained by the model) is orthogonal, in the sense of the selected inner product, to the range of the operator $\bar{\bar{A}}$. The uniqueness of the solution is not coincidental. It is due to the fact that the spaces $R(\bar{\bar{A}})$ and $N(\bar{\bar{A}}^T)$ are complementary. The data space R^m represents the direct sum of these two spaces (a vector $\Delta \vec{d}^m \in R^m$ has a unique representation as the direct sum of $\Delta \vec{d}^c \in R(\bar{\bar{A}})$ and $\Delta \vec{d}^m - \Delta \vec{d}^c \in N(\bar{\bar{A}}^T)$).

In our work, the observables will be projected on the linearized core model according to the criterion introduced in Eq. (3-28). Note that if the weights $\{\Lambda_i\}$ in Eq. (3-25) are all equal to a certain value γ , (*i.e.* $\bar{\bar{A}} = \gamma \bar{\bar{I}}$; and $\bar{\bar{I}} \in R^n$ is the identity matrix), one would be calculating a version of the Euclidean length scaled by $\sqrt{\gamma}$. Distinct weights will give rise to *oblique* projection (‘oblique’ in the sense of our 3-D visualization of orthogonality). The weights are usually determined by the uncertainty information (covariance data), or any

special weights assigned to the measured observables. Figure 3.3 illustrates how the measured observables $\Delta \vec{d}^m$ are projected on the model $R(\bar{\bar{A}})$ according to different weights $\{\Lambda_j\}$ and how that results in different “closest matches” $\Delta \vec{d}^c$ to the measured observables $\Delta \vec{d}^m$.

3.3. Adapting the Core Simulator Model

After this short tour of definitions, let us formulate the linearized version of the discrete inverse problem of given certain measured core attributes and our corresponding best knowledge about core parameters, how can we adapt that best knowledge of those parameters to get the best match between the predicted and measured core attributes[3]. The notion of “best”, within the context of our application, refers to the required high fidelity and robustness of the adaption.

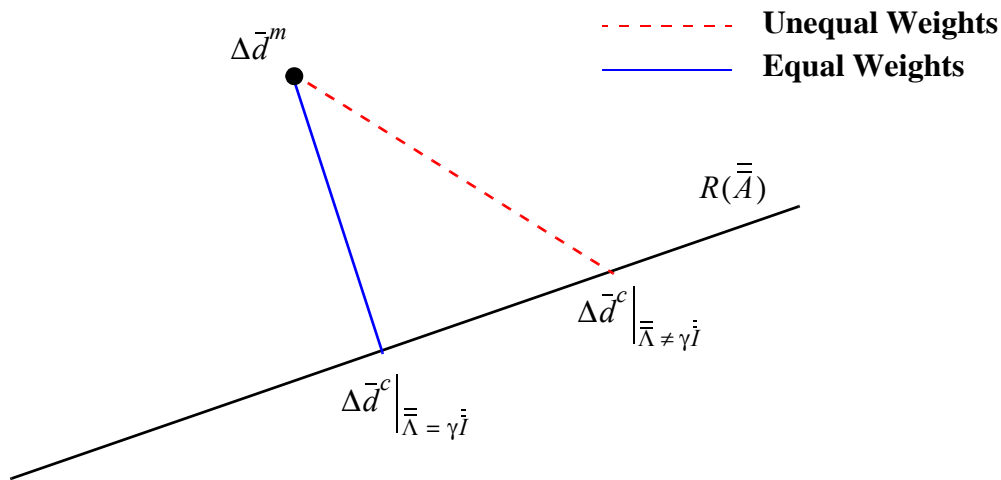


Figure 3.3: Projection of the Measured Observables onto the Linearized Core Model (Different $\bar{\bar{\Lambda}}$ Matrices).

3.3.1 Model Linearization

Let \bar{d}^m and \bar{d}^c be vectors of dimension m whose components refer to the measured and predicted core observables, respectively, $\bar{d}^m, \bar{d}^c \in R^m$ and R^m refers to the data (observables) space. Let $\bar{\lambda}^m$ and $\bar{\lambda}^c$ be two vectors of dimension l whose components are the measured and calculated steady state core reactivity (e.g. k_{eff}) at selected burnup points during cycle life (note that $\bar{\lambda}_j^m|_{j=1,l} = 1$ for actual plant data at all times during the cycle, assuming measurements were completed at steady state power conditions). These discrete burnup points are referred to as “time steps”. Let n_d be the total number of LPRM readings in the core and assume that $n_d = m/l$, (e.g. n_d measured observables are recorded at each time step). Let the core design basis simulator model be represented by the two vector nonlinear equations,

$$\bar{d}^c = \vec{\Theta}(\bar{p}), \quad (3-29)$$

$$\bar{\lambda}^c = \vec{\Pi}(\bar{p}), \quad (3-30)$$

where \bar{p} is a vector of dimension n whose components represents the model parameters, $\bar{p} \in R^n$ and R^n refers to the parameters space.

Within the context of our application, the core parameters and their a priori information are given by,

$$\bar{p} = \left[f^{c_3} f^{k_3} \{f_1^{n,j}, f_2^{n,j}\} \right]^T, \text{ and } \bar{p}_\infty = \left[\hat{f}^{c_3} \hat{f}^{k_3} \{\hat{f}_1^{n,j}, \hat{f}_2^{n,j}\} \right]^T, \text{ respectively.} \quad (3-31)$$

The measured and predicted core observables are given by,

$$\vec{d} \Big|_{j=m,c} = \left[\vec{d}_1^j \ \vec{d}_2^j \ \dots \ \vec{d}_{n_d}^j \ \vec{d}_{n_d+1}^j \ \vec{d}_{n_d+2}^j \ \dots \ \vec{d}_{2n_d}^j \ \vec{d}_{2n_d+1}^j \ \dots \vec{d}_{ln_d}^j \right]^T. \quad (3-32)$$

Eq. (3-29) and Eq. (3-30) can be linearized around a reference point $(\vec{d}_0^c, \bar{\lambda}_0^c, \bar{p}_0)$ where

$\vec{d}_0^c = \bar{\Theta}(\bar{p}_0)$ and $\bar{\lambda}_0^c = \bar{\Pi}(\bar{p}_0)$, to give:

$$\vec{d}^c = \vec{d}_0^c + \bar{\bar{A}}(\bar{p} - \bar{p}_0) + \text{Higher Order Terms}, \quad (3-33)$$

and

$$\bar{\lambda}^c = \bar{\lambda}_0^c + \bar{\bar{B}}(\bar{p} - \bar{p}_0) + \text{Higher Order Terms}, \quad (3-34)$$

where the Jacobian matrices $\bar{\bar{A}}$ and $\bar{\bar{B}}$ are defined by

$$[\bar{\bar{A}}]_{ij} = \frac{\partial}{\partial \bar{p}_{0j}} \bar{\Theta}_i(\bar{p}_0), \quad [\bar{\bar{B}}]_{ij} = \frac{\partial}{\partial \bar{p}_{0j}} \bar{\Pi}_i(\bar{p}_0), \quad (3-35)$$

with $\bar{\bar{A}} \in R^{m \times n}$ and $\bar{\bar{B}} \in R^{l \times n}$, and i and j refer to the i th predicted observable and j th model parameter, respectively, at the reference conditions.

3.3.2 Least-Squares Approach

After linearizing the core simulator model, the model parameters are adapted to reduce the disagreement between the measured and predicted observables. That adaption is accomplished by utilizing a least-squares approach in which $\Delta \bar{p}$ is selected iteratively,[36],[42],

$$\Delta \bar{p} = \sum_{k=1}^{\text{convergence}} \Delta \bar{p}_k,$$

to minimize a quadratic form, for an iterate¹ k , that is given by,

$$S(\bar{d}_k^c) = \|\bar{d}^m - \bar{d}_k^c\|_{\bar{C}_d}, \quad (3-36)$$

subject to:
$$\bar{d}_k^c = \bar{d}_{k-1}^c + \bar{A}(\bar{p}_k - \bar{p}_{k-1}),$$

where
$$\bar{d}_{k-1}^c = \bar{\Theta}(\bar{p}_{k-1}) \quad \text{and} \quad \Delta \bar{p}_k = \bar{p}_k - \bar{p}_{k-1}.$$

This can be re-written as,

$$S(\Delta \bar{d}_k^c) = \|\Delta \bar{d}_k^m - \Delta \bar{d}_k^c\|_{\bar{C}_d}, \quad (3-37)$$

subject to:
$$\Delta \bar{d}_k^c = \bar{A} \Delta \bar{p}_k,$$

where \bar{C}_d is a weighting matrix for observables, and $\Delta \bar{d}_k^m = \bar{d}^m - \bar{d}_{k-1}^c$ and

$\Delta \bar{d}_k^c = \bar{d}_k^c - \bar{d}_{k-1}^c$ both measure the difference between the observables and a certain

reference point in the data space. However, for convenience, \bar{d}_k^m and $\Delta \bar{d}_k^m$ or \bar{d}_k^c and $\Delta \bar{d}_k^c$

will both refer to the observables and will be used interchangeably without confusion.

To find $\Delta \bar{p}_k$, one utilizes the least-squares normal equations formulation which is given by:

1. Jacobian matrices do not have k dependence. In current work, the sensitivity coefficients are calculated by brute force (*i.e.* numerical differentiation). However, since the number of the adjusted parameters is too large, that results in a huge computational burden to determine the sensitivity coefficients and re-evaluate them at each iteration of the search. 40 minutes are required on a 700 MHZ PC, to burn the core we utilized in our work (a BWR/6 core with 724 fuel assemblies) using core follow data. For the sake of simplicity and for exploratory purposes, we decided to use a Quasi-Newton search, evaluating sensitivity coefficients at only the initial reference conditions and not updating them as the iterative search progress. This decreases the likelihood of convergence and if convergence occurs, the rate of convergence could be considerably slower depending on the nonlinearity of the core simulator model. However, the main focus of this work is not whether the search will or will not converge, but how accurate, regularized and robust the results are. Fortunately, it was found that the Quasi-Newton search always lead to convergence, perhaps because the sizes of the perturbations introduced into the design basis core simulator are sufficiently small.

$$\Delta \bar{p}_k = [(\bar{A}^T \bar{C}_d \bar{A})^{-1} \bar{A}^T \bar{C}_d] \Delta \bar{d}_k^m, \quad (3-38)$$

if the problem is over-determined and \bar{A} has a full column rank, or

$$\Delta \bar{p}_k = [\bar{C}_p \bar{A}^T (\bar{A} \bar{C}_p \bar{A}^T)^{-1}] \Delta \bar{d}_k^m, \quad (3-39)$$

if the problem is under-determined and \bar{A}^T has a full column rank, where \bar{C}_p is a weighting matrix for the parameters. The more general situation, which is the case in our problem, when \bar{A} or \bar{A}^T does not have a full rank will be discussed in the next section in a more qualitative way for simplicity.

3.3.3 Geometrical Interpretation of Least-Squares Solution and Its Deficiencies

In light of the discussion presented in the previous section, the geometrical interpretation of the least-squares solution for an iterate $\Delta \bar{p}_k$ can be described as follows: Find the core parameters' adjustment $\Delta \bar{p}_k$ which maps into the data space to a point $\Delta \bar{d}_k^c$ on $R(\bar{A})$ that is closest in the sense of \bar{C}_d to measured observables $\Delta \bar{d}_k^m$. That can be considered, as mentioned before, as an oblique projection of $\Delta \bar{d}_k^m$ on $R(\bar{A})$ whose angle is determined by \bar{C}_d . According to that projection, $\langle \Delta \bar{d}_k^m - \Delta \bar{d}_k^c, \bar{A} \Delta \bar{p}_k \rangle_{\bar{C}_d} = 0$ (e.g. $\Delta \bar{d}_k^m - \Delta \bar{d}_k^c$ is orthogonal to $R(\bar{A})$ in the sense of \bar{C}_d). To perform this least squares adaption, the vector of observables is projected on the range of the operator \bar{A} (in the sense of \bar{C}_d). That projection is mapped back from the data space to the parameters space such as an additional criterion on model parameters that must be satisfied. For example, require that the solution vector $\Delta \bar{p}_k$ be

orthogonal to the null space of the operator $\bar{\bar{A}}$ (minimum norm solution). The angles of projection in the data and the parameter spaces are determined according to the matrices $\bar{\bar{C}}_d$ and $\bar{\bar{C}}_p$, respectively. Note that the different components of the data and parameters vectors are amplified by different multipliers determined by the matrix $\bar{\bar{A}}$ (e.g. singular values) when mapped back and forth between the data and parameters space. The first projection is necessary, since it removes that part (component) of the observables which is orthogonal (in the sense of $\bar{\bar{C}}_d$) to the range of the mathematical operator $\bar{\bar{A}}$ (e.g. that part which cannot be explained by the mathematical model used to represent our physical phenomena of interest). That component of the observables is either due to some noise on measured observables, or due to some unexplained aspects of our physical phenomena. The second projection (in the sense of $\bar{\bar{C}}_p$) is however arbitrary from a mathematical point of view, since any information about the parameters (components) in the null space of $\bar{\bar{A}}$ will not be mapped to the data space, (e.g. vanished [multiplied by zero] and will not be reflected in the data). However, from a physical point of view, the observables we are collecting might not contain information about that part (component) of the parameters which is not mapped to the data space. That does not necessarily mean that if one analyzed another set of observables, that component of the parameters will not be mapped to the new data space under the new mapping. Including these unmapped information about model parameters is then very crucial to the robustness of the adaptive techniques.

3.3.4 Sources and Consequences of Ill-Conditioning

In the current work, the main sources of the ill-conditioning were attributed to two factors: 1) Sensitivity coefficients of the adjusted parameters differed by orders of magnitude (reflected in the singular values of the matrix $\bar{\bar{A}}$), so the information about these parameters with low sensitivities is not effectively mapped to the data space (*e.g.* reducing the information content of the data signal¹), specially when the noise level becomes large enough compared to this information. 2) Some of the adjusted parameters have similar sensitivity profiles. These two factors result in reducing the effective rank of the matrix $\bar{\bar{A}}$. In our application, the least-squares problem is overdetermined; however it is ill-conditioned. In this case, the adjusted parameters will be very sensitive to the noise, since those effectively vanishing or unmapped components of the parameters will be estimated based on the noise level in the data space, which leads to a totally unphysical, unrobust and random (*i.e.* nonunique) adaption. Figure 3.4 illustrates that situation, where the observables with the noise associated with them are mapped back to the parameters space[42]. For illustration purposes, the near null spaces and effective ranges of the operator and its transpose are referenced. Since the near null space of $\bar{\bar{A}}$ is not empty, that leads to an effectively nonunique solution.

3.3.5 Regularized Least Squares Problem

To solve the previously mentioned problem, one defines a new transformation which maps those effectively unmapped information about model parameters to a new expanded data space, where now the observables would contain information about model parameters

1. Refer to Appendix A for a qualitative discussion of the definition of “Data information content”.

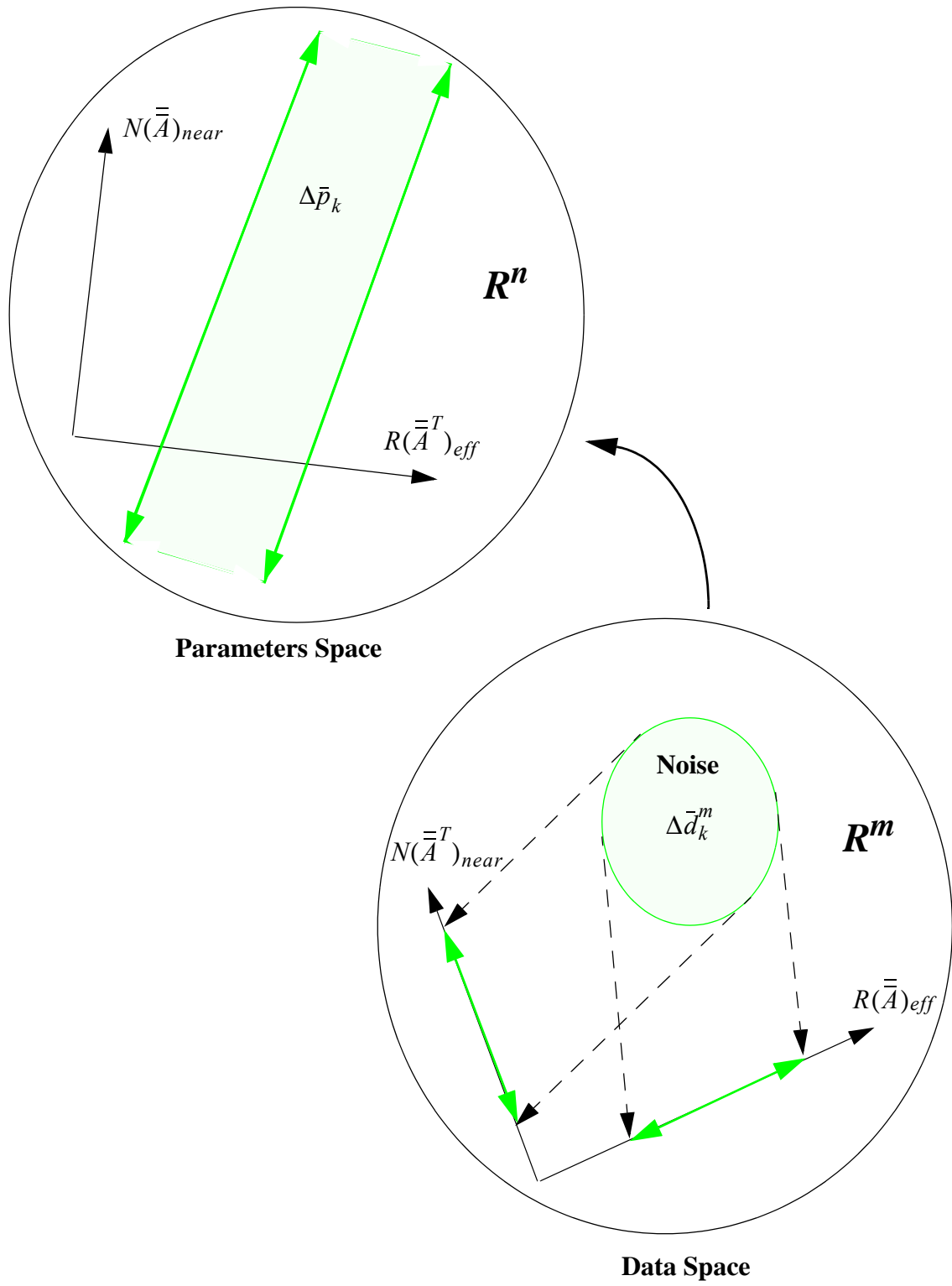


Figure 3.4: Inverse Mapping of Information in a 'Discrete Ill-Posed System'.

sufficient to cast the problem into a well-conditioned one, (*i.e.* the data components carrying information about model parameters are not masked by the presence of noise). Regularization is a set of mathematical techniques which is utilized in defining a new transformation to cast an ill-posed problem into a well-posed one. One way to do this is by supplying a priori information about model parameters. That can take several forms like¹:

$$\bar{p}_k = \bar{p}_\infty, \quad (3-40)$$

$$\bar{\bar{B}}(\bar{p}_k - \bar{p}_{k-1}) = \bar{\lambda}^m - \bar{\lambda}_{k-1}^c. \quad (3-41)$$

Eq. (3-40) may define historical best known values for the model parameters. Eq. (3-41) defines certain relationships the parameters should satisfy (*i.e.* criticality constraints in our case). This additional information can be added to those given by Eq. (3-33) in two different ways. In the first way, one can incorporate all the information in a single least-squares minimization problem and different weights can be assigned to different pieces of information about model parameters. That leads to a problem of the form, written in a least-squares sense:

$$\begin{bmatrix} \bar{\bar{A}} \\ \mu_1 \bar{\bar{I}} \\ \mu_2 \bar{\bar{B}} \end{bmatrix} (\bar{p}_k - \bar{p}_{k-1}) = \begin{bmatrix} \bar{d}^m - \bar{d}_{k-1}^c \\ \mu_1 (\bar{p}_\infty - \bar{p}_{k-1}) \\ \mu_2 (\bar{\lambda}^m - \bar{\lambda}_{k-1}^c) \end{bmatrix}, \quad (3-42)$$

where μ_1 and μ_2 are scalar weights. This is equivalent to a minimization problem of a quadratic form given by, for an iterate k ,

$$S(\bar{d}_k^c, \bar{p}_k) = \|\bar{d}^m - \bar{d}_k^c\|_{\bar{\bar{C}}_d}^2 + \mu_1^2 \|\bar{p}_k - \bar{p}_\infty\|_{\bar{\bar{C}}_p}^2 + \mu_2^2 \|\bar{\bar{B}}(\bar{p}_k - \bar{p}_{k-1}) - (\bar{\lambda}^m - \bar{\lambda}_{k-1}^c)\|^2, \quad (3-43)$$

subject to the linearized core model given by:

1. These special forms are used to directly serve the discussion.

$$\bar{d}_k^c = \bar{d}_{k-1}^c + \bar{A}(\bar{p}_k - \bar{p}_{k-1}).$$

In the second way, some of the additional information is utilized as constraints, which have to be exactly satisfied versus in a least-squares sense. In our problem, this information represents the criticality constraint defined by Eq. (3-41). In this case, the search can be formulated to be a minimization problem of the quadratic form¹,

$$S(\bar{d}_k^c, \bar{p}_k) = \|\bar{d}^m - \bar{d}_k^c\|_{\bar{C}_d}^2 + \mu^2 \|\bar{p}_k - \bar{p}_\infty\|_{\bar{C}_p}^2, \quad (3-44)$$

subject to the linearized and constrained core model given by:

$$\bar{d}_k^c = \bar{d}_{k-1}^c + \bar{A}(\bar{p}_k - \bar{p}_{k-1}) \quad \text{and} \quad \bar{B}(\bar{p}_k - \bar{p}_{k-1}) = \bar{\lambda}^m - \bar{\lambda}_{k-1}^c,$$

where μ is a scalar weight. Figure 3.5 is a two dimension plot of the observables and parameters space. The task of the adaption (least-squares minimization problems of Eq. (3-43) or Eq. (3-44)) is to iteratively find the closest point on the model (\bar{d}^c, \bar{p}) to the point which represents our best available information about observables (measured quantities) and model parameters $\bar{d}^m, \bar{p}_\infty$.

1. In general, one would minimize a quadratic function of the form[43]-[44],

$$S(\bar{d}_k^c, \bar{p}_k) = \begin{bmatrix} \bar{d}^m - \bar{d}_k^c \\ \bar{p}_k - \bar{p}_\infty \end{bmatrix}^T \begin{bmatrix} \bar{C}_d & \bar{C}_{dp} \\ \bar{C}_{dp}^T & \mu^2 \bar{C}_p \end{bmatrix} \begin{bmatrix} \bar{d}^m - \bar{d}_k^c \\ \bar{p}_k - \bar{p}_\infty \end{bmatrix}.$$

However, within the context of our application the matrices \bar{C}_{dp} and its transpose \bar{C}_{dp}^T will be assumed to be zero. That is equivalent to assuming that the a prior knowledge of the input parameters doesn't depend on how the experimental evaluation of the observables are made, which is a sound assumption [36].

3.3.6 Determination of the Regularization Parameters and Weighting Matrices

The scalar weights μ_1 , μ_2 and μ are referred to as regularization parameters, and the associated regularization technique is called Tikhonov Regularization. It represents one of the most common and utilized regularization techniques. Different approaches offer different ways to determine the optimum values for these parameters based upon different criteria. For the current work, we determined their optimum values experimentally, by “trial and error”¹. In

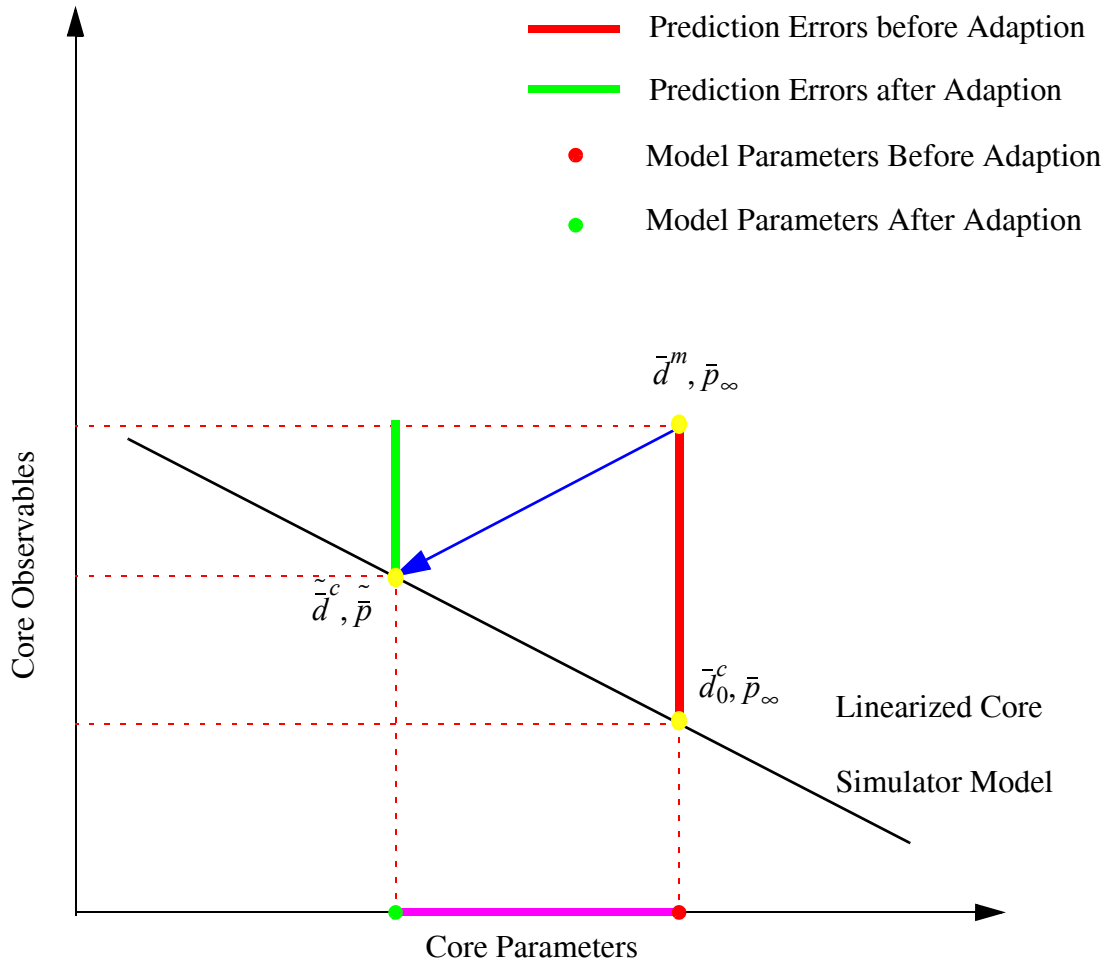


Figure 3.5: Supplying A Priori Information about Model Parameters.

1. Refer to Appendix B for more details.

any of these regularized forms of either Eq. (3-43) or Eq. (3-44), the term $\|\bar{d}^m - \bar{d}_k^c\|_{\bar{C}_d}$ is referred to as the misfit term, and the term $\|\bar{p}_k - \bar{p}_\infty\|_{\bar{C}_p}$ or $\|\bar{B}(\bar{p}_k - \bar{p}_{k-1}) - (\bar{\lambda}^m - \bar{\lambda}_{k-1}^c)\|$ is referred to as the regularized term. The minimized quadratic form is a weighted sum of these two different kinds of terms. If the selected regularization parameter approaches zero, the problem reduces to the previous least squares case and the parameters' adjustment are mainly determined by the observables; whereas, if the regularization parameter approaches infinity, the first term (data misfit) is negligible with respect to the second term (regularized), and the parameters are mainly determined by the a priori information and the constraints, if any.

The weight matrices utilized in this study are given by:

$$\bar{C}_d = \bar{I} \bar{\Lambda} \bar{I}^T = \bar{\Lambda} = \begin{bmatrix} \bar{\Lambda}_1 & & & \\ & \bar{\Lambda}_2 & & \\ & & \ddots & \\ & & & \bar{\Lambda}_i & \\ & & & & \ddots \\ & & & & & \bar{\Lambda}_l \end{bmatrix}^{m \times m}; \quad \bar{\Lambda}_i = \gamma_i \bar{I}_d,$$

$$\bar{C}_p = \bar{I}_p,$$

where $\bar{I}_d \in R^{n_d \times n_d}$ and $\bar{I}_p \in R^{n \times n}$ are the identity matrices, and $\{\gamma_i\}_{i=1,l}$ are weights given to the observables recorded at different burnup steps and are given by,

$$\gamma_i = \frac{Bu_i}{Bu_{EOL}} \times \frac{\Delta Bu_i}{Bu_{EOL}}; \quad \Delta Bu_i = Bu_i - Bu_{i-1}, \quad (3-45)$$

where Bu_i and Bu_{EOL} are the accumulated burnup after i time steps and the total cycle accumulated burnup, respectively. Note that the prediction errors are expected to be functions of cycle burnup. The weight for a certain time step is selected to be proportional to the relative amount of burnup increment for that time step, which if the plant were at full power, is the relative time the error exists. It is also more important to accurately predict core behaviour (*i.e.* core criticality) at EOL than at BOL. To do that, a simple linear proportionality was assumed with cycle burnup.

The covariance information about model parameters are not included in the current study. The search for the optimum model parameters $\tilde{\bar{p}}$ was completed[45] using the approach suggested by Eq. (3-43). The variables \bar{p}_∞ and $\tilde{\bar{p}}$ refer to the a priori and a posteriori information about model parameters (*e.g.* before and after the adaption), respectively, where

$$\tilde{\bar{p}} = \left[\tilde{f}^{c_3} \tilde{f}^{k_3} \{ \tilde{f}_1^{n,j}, \tilde{f}_2^{n,j} \} \right]^T. \quad (3-46)$$

3.3.7 Tuning of Adaptive Techniques

The *oblique* projection of the a priori knowledge about model parameters and measured observables on the core model is determined by three factors: 1) Regularization parameters, 2) covariance information of the estimated model parameters and measured observables, in addition to 3) any specialized form of weights imposed on the search to serve certain technical interests (*i.e.* burnup weights). These three factors should be tuned simultaneously to obtain the most acceptable robust estimate of model parameters which will result in a better agreement between measured and predicted core attributes, while still constraining model parameters' adjusted values to a range about their best known (a priori)

values defined by their uncertainties (*i.e.* statistically consistent with their a priori information).

4. Cases Studied, Results and Conclusions

A demonstration of different test cases will be provided in this chapter. The test cases were selected such as to serve various purposes. First, to give insight into the machinery of the proposed adaptive techniques and show that regularization results in a physical adaption of the core simulator which is consistent with core physics. Second, to explore the potential of adaptive techniques to accurately predict core observables recorded at future times, based on an ‘adapted design basis core simulator’, denoted by AC, which utilizes current and past measurements. As emphasized before, the main issue that needs to be assessed in any proposed adaptive technique is checking the robustness and fidelity of the adapted models. For that purpose, different approaches and/or criteria will be utilized to measure, in a qualitative and/or quantitative sense, the robustness and fidelity of each of the adapted test cases. The study has been conducted for a BWR/6 reload core containing 724 fuel bundles. The cycle burnup for the selected core is 8579.20 MWD/STU. Figure 4.2 shows the control rod pattern during cycle life. The experimental observables consisted of the readings of 44 LPRM detector strings positioned throughout the core in channels which do not contain control rods, where each string consists of 4 axial detectors as shown in Figure 4.1¹.

At this early stage of project development, the virtual approach will be employed where two different versions of the core simulators are utilized, one to represent the actual plant data and the other a core simulator that would be used by analysts. The version of the core simulator, referred to as the ‘virtual core’, denoted by VC, is used to represent actual

1. Not to scale.

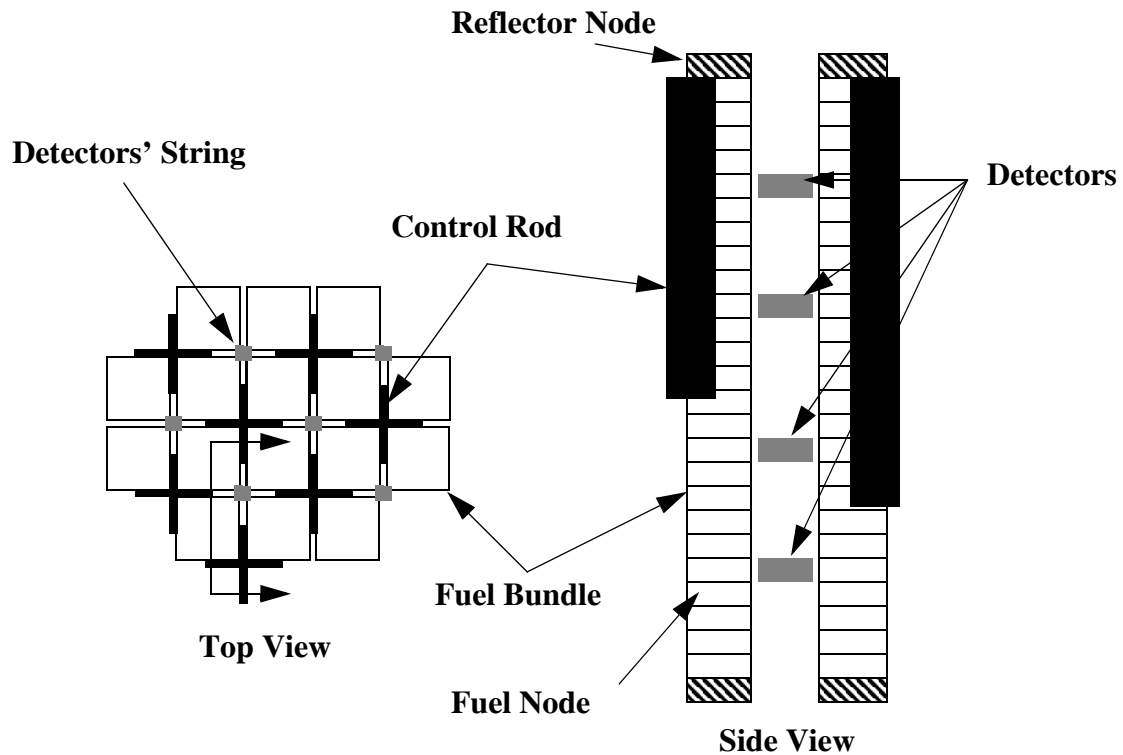


Figure 4.1: Detectors' Layout.

plant data. That version corresponds to the current version of a selected core simulator (*e.g.* FORMOSA-B). The virtual core is utilized to simulate detectors' signals (observables) which are used to adapt another version of the same core simulator. The version of the core simulator used by analysts is a modified version of the virtual core, where now errors are deliberately introduced in its modeling. That version is referred to as the 'design basis core simulator', and is denoted by DC. The errors introduced give rise to discrepancies between the VC and the DC's predictions of different core attributes. The errors were selected such as these discrepancies are representative of the actual discrepancies which exist between actual plant data and existing core simulators. Two types of errors were simulated in the virtual core

approach, modeling and input data errors. Modeling errors were introduced by utilizing the Lellouche-Zolotar EPRI methodology for the VC versus the Zuber-Findlay void-quality correlation for DC. Two different approaches for adapting the core have been studied. In the first approach, denoted by AC1, thermal-hydraulics and cross-sections input data were both adapted to enhance the agreement between the DC and VC. In the second approach, denoted by AC2, only cross-sections input data were adapted. Input data errors were introduced by randomly selecting all the core parameters, whether they are adapted or not (*e.g.* all f factors) from normalized Gaussian distribution with a 1% standard deviation. The perturbed values (*e.g.* \hat{f}^{c_0} , \hat{f}^{k_3} , and $\{\hat{f}_1^{n,j}, \hat{f}_2^{n,j}\}$) are assumed to represent our best knowledge about the core parameters. Adaption was always completed at the rated conditions of power and flow rates, and the search is constrained by incorporating the criticality constraints in a least-squares sense in the quadratic function to be minimized, see Eq. (3-43).

Different approaches have been taken to see how well the adaption can identify and explicitly adjust for different sources of errors, and to show its potential for those cases when adaption is performed on the wrong parameters. To differentiate initially (*e.g.* before adapting the core), in a qualitative sense, between the two simulated types of error sources and their respective magnitudes, a comparison is made of the VC to the DC response when input data errors were and were not present. Also compared are the AC to the VC response with and without LPRM signal noise, with the VC associated data used in the adaption always containing noise. That step was taken to see how well adaptive techniques can be used to filter out instrument noise.

Figure 4.3 compares the LPRM RMS and core reactivity errors of the DC before and after adaption using the two approaches, AC1 and AC2, for three different cases. For case AC1-F, the recorded detectors' signals and criticality constraints at all burnup steps (*e.g.* l time steps) are included in the adaption, hence denoted 'F' for full. For case AC1-H only the observables recorded at half of the total number of time steps (*e.g.* $l/2$), selected at random, are utilized to adapt the core, hence denoted 'H' for half. Approach AC2 has been utilized only for case AC2-F. Each of the figures showing the LPRM RMS errors consists of four sets of graphs as now explained: Graph (a) presents the RMS error between the VC, which includes

Table 4.3: Figures' nomenclature.

Symbol	Interpretation
AC1	AC utilizing approach 1, in which the thermal-hydraulics and reactor physics data are adapted.
AC2	AC utilizing approach 2, in which the reactor physics data are adapted.
-F	All observables' signals are utilized in adaption.
-H*	Half of the observables' signals are utilized in adaption.
-1T*	One third of the observables' signals are utilized in adaption.
-2T*	Two third of the observables' signals are utilized in adaption.
<I>	Calculated errors accounts for input data errors.
<M>	Calculated errors accounts for modeling errors.
RV	Rated Void Fractions, (<i>i.e.</i> rated conditions).
HV	High Void Fractions, (<i>i.e.</i> decreased flow rates)
LV	Low Void Fractions (<i>i.e.</i> increased flow rates and decreased power)
Acc. Burnup	Accumulated Burnup

* See text for more details on how these subsets of observables' signals are selected

the instrument noise, and the DC's predictions before adaption, where the errors are calculated based on the simulation of both modeling (M) and input data (I) errors. Graph (b) calculates RMS errors in the same fashion as Graph (a), except now only modeling errors (Zuber-Findlay void-quality correlation) were introduced in the DC. Graph (c) presents the RMS error between the VC and the DC after the adaption has been completed. Graph (d) determines the RMS errors in the same fashion as Graph (c), except now noise is not incorporated in the VC responses. Qualitatively, Graph (a) and Graph (b) show that the initial individual contribution of each source of error, modeling errors and input data errors, are approximately of the same magnitude. Graph (c) shows that the differences in LPRM signals between the AC and the VC are of the order of the noise level. The RMS errors in Graph (d) are presented without the noise, showing that the AC and the VC LPRM signals agree well, (adaption can be potentially utilized as a powerful noise filter). Core reactivity errors are also presented to show how powerful the adaption is in accurately reducing the prediction uncertainties in the k_{eff} values to about one order of magnitude less than their original values before adaption. By comparing case AC1-F and case AC1-H, one finds that the order of prediction errors for all the detectors' signals and the criticality constraints are the same whether they are or are not included in the adaption, which confirms the physical nature of the adaption.

Case AC2-F also shows as good agreement as with either case AC1-F or AC1-H. That's to be expected, since as mentioned before, the adapted core parameters will account for both the input data errors and the modeling errors at which the adaption was completed. However, one would think that by using approach AC2, the agreement between the VC and DC will be degraded when trying to predict core behaviour at different flow conditions (*i.e.*

different void fractions). With the availability of a VC, one can compute the response of the core at different operating conditions other than the rated conditions. As mentioned above, one can think of the case when the Zuber-Findlay void-quality parameters are adapted, as providing the adaption with the freedom to adjust to not only input data errors but also modeling errors separately. So if the core is operating at higher or lower void fraction, the prediction errors of approach AC1 would be expected to be less than those of approach AC2. To attain higher void fractions, denoted by HV, in the core, the flow rates were uniformly reduced throughout the cycle life to 80%, and to attain lower void fractions, denoted by LV, the flow rates and power were uniformly changed to 110% and 90%, respectively, of their rated values, denoted by RV. Figure 4.4 shows the power to flow ratio during cycle life for the three studied cases, (*e.g.* RV, HV, and LV). Figure 4.5 and Figure 4.6 compare the LPRM signals' prediction errors for the HV and LV cases, respectively, for two different adaptive approaches: AC1-F and AC2-F. The results show that the LPRM RMS errors obtained using approach AC2-F are at least two times larger than those errors obtained when using approach AC1-F. That confirms that approach AC1-F corrects more explicitly for modeling errors and input data errors than approach AC2-F, giving rise to a more robust adaption.

To further confirm this, we utilize a more quantitative comparison test in which different criteria are used to calculate the LPRMs RMS and core reactivity errors. This was accomplished by re-calculating the initial and final errors (*e.g.* before and after adaption) but now utilizing the Lellouche-Zolotar EPRI methodology for the DC. Note that when calculating the LPRMs RMS errors, noise was not included in the VC signal. In this manner, the effect of cross-section input data errors could be isolated. In Figure 4.7, Graph (a) presents the re-calculated initial errors of the DC, and Graph (b) and Graph (c) present the re-calculated

errors of the AC utilizing approaches AC1-F and AC2-F, respectively. Sets of sub-figures present the three previously mentioned cases of core conditions (*i.e.* RV, HV, and LV), respectively. Graph (a) and Graph (c) show that the adaption generally reduces the DC errors due to initial input data errors, even though the adaption is based on the Zuber-Findlay void-quality correlation, and the comparison is based on the Lellouche-Zolotar EPRI methodology. Hence, we can conclude that the adaption is mainly reducing the prediction errors due to input data errors separately from those due to modeling errors. However, when one analyzes Graph (c) where the void-quality parameters are not adapted (*e.g.* Approach AC2), one observes that the errors of the AC2 now are even larger than the initial errors, which indicates that the adaption is highly affected by the magnitude and type of the modeling errors at which the adaption was completed. One should also notice that when using DC to predict core behaviour at LV, that leads to a reduction in the predictions errors since there is less voiding in the core, and consequently the size of the prediction errors due to modeling errors will be reduced (see Graph (a) and Graph (b), AC2-F in Figure 4.5 and Figure 4.6). Comparing the size of the initial prediction errors for the LV case (see Graph (b), LV in Figure 4.7), it is observed that the prediction errors are of the same magnitude as when using the AC1 to predict core behaviour at LV (see Graph (d), AC1-F in Figure 4.6), with the latter of somewhat smaller size, since adaption reduced input data errors. So, whether one uses the Lellouche-Zolotar EPRI methodology or the Zuber-Findlay void-quality correlation for the AC to predict core conditions at LV, one obtains the same magnitude of LPRMs RMS and reactivity errors. This confirms also that the adaption only corrects for input data errors, and is not affected by how much voiding is present when the core is adapted at rated conditions.

In realistic situations, one would be interested in adapting the DC based on the current core observables and utilizing the AC to predict future core attributes, including core observables. To demonstrate that situation, two other test cases have been conducted, where now core observables recorded at only one third, denoted by AC1-1T, and two thirds, denoted by AC1-2T, of core cycle have been used in the adaption. The AC is then utilized to predict core behaviour over the entire cycle. Figure 4.8 compares the predictions of the core observables and the core reactivity of the VC and the AC for both cases AC1-1T and AC1-2T, in a similar fashion to the results demonstrated before. It is observed that for both cases, the adaptive techniques are still capable of adjusting for errors in modeling and accurately predicting core behaviour over the entire cycle. It is important to mention here, that when less information is utilized to adapt the DC, the problem becomes more ill-conditioned and the effective rank of the least-squares associated matrix reduces accordingly with the amount of information employed in adaption. However, the relatively small prediction errors indicate that the regularized adaptive techniques are capable of limiting the adaption to physical situations¹. When one carefully compares those two case with case AC1-F of Figure 4.3, one notices that the LPRM RMS errors for both cases AC1-1T and AC1-2T are monotonically increasing with burnup (*i.e.* following a certain pattern) for the portion of the cycle whose observables' were not included in the adaption. For case AC1-1T, core reactivity is predicted over the entire cycle to a better degree of accuracy than AC2-2T. For case AC2-2T, core reactivity errors are higher at EOC and BOC than at the middle of the cycle. Several observations can be made accordingly. First, it is apparent that some aspects of the core

1. In general, different regularization parameters are utilized depending on the ill-conditioning of the problem.

behaviour start building up later in the cycle, and consequently no information about these phenomena appears in the observables signals utilized to adapt the DC. Hence, no adaption is made to adjust for these phenomena since, in this case of lack of information, adaption confines the adjusted parameters to the a priori information about these parameters. Second, by recalling that the adaption favors (gives more weight) to observables recorded at higher burnups than those at lower burnups, see Eq. (3-45), the poorer behaviour of case AC2-2T in predicting core reactivity, suggests that the burnup functionalization utilized is not adequate enough to adjust for these errors and hence more sophistication is necessary. By analyzing the core reactivity errors, we are able to make a more educated guess on how to functionalize core parameters in terms of cycle burnup.

Figure 4.9 shows the a priori and a posteriori information about model parameters (*e.g.* the f factors, the components of \bar{p}_∞ and \tilde{p} , respectively) for three different levels of regularization. The second case corresponds to the highest fidelity and robustness adaption. Recall that the a priori values of core parameters (*e.g.* the f factors) were determined by randomly perturbing their true values using a normal Gaussian distribution whose standard deviation equals 1% (*e.g.* the uncertainty of the a priori information is 1% for all core parameters). It is observed that the a posteriori information about core parameters is statistically consistent with the a priori information for case (b) and case (c). For strong regularization, case (c), the a posteriori information approaches the a priori information and effectively no adaption is performed. For weaker regularization, case (a), the a posteriori information, for an ill-conditioned problem, has larger uncertainty in general, since the adaption is affected more by the noise level in the observables' signals. Note that, if the

problem is well-conditioned, the a posteriori uncertainty information about core parameters is expected to be less than the a priori uncertainty information, if the measured observables uncertainty (due to noise) is less than the predictions uncertainty (due to input data errors, assuming exact modeling). For an intermediate level of regularization, case (b), a compromise is achieved where now, the pieces information about model parameters which are mapped effectively between the data (observables) and the parameter space (*i.e.* that information associated with large singular values), their uncertainty level is mainly determined by the observables uncertainty. However, for those pieces of information which are effectively vanished (due to the small singular values), their a posteriori uncertainty information is mainly determined by the a priori information about model parameters. Note also that the thermal-hydraulic parameter (C_0) has an adjusted value that deviates 6% from its true value of 1.0. This is to be expected since the functionalization of the void is not consistent with reality (*i.e.* using the observables produced by the Zuber-Findlay void-quality spatially independent parameters to attempt to match the Lellouche-Zolotar void-quality spatially dependent parameters). The thermal-hydraulic parameter (C_0) has a strong sensitivity profile (*i.e.* its sensitivity profile is large in magnitude and different from other model parameters' sensitivity profiles), and hence its adjustment is mainly determined by the observables for different levels of regularization; however, the second thermal-hydraulic parameter (k_3) has a very weak sensitivity profile, and its adjusted value is mainly determined by the a priori information.

The same regularization parameters are used to restrict the search for all model parameters to their a priori values. The choice of the magnitudes of the regularization parameters affects how far the a posteriori information about core parameters is from the a

priori information, since it affects the trade-off between the regularized term and the data misfit term of the quadratic function to be minimized. That trade-off should depend on how much information about core parameters is contained in the observables' signals. The information content of the observables' signals depend on the conditioning¹ of the linearized core model, represented by the matrix operator $\bar{\bar{A}}$. Appendix B discusses the L-curve which we utilized to determine the optimum regularization parameters and hence degree of conditioning. Using the same regularization parameters to limit the adjustments for all core parameters can be considered as a first logical assumption² since the a priori uncertainty information about core parameters is assumed to be of the same magnitude (*i.e.* 1%). In general, the compromise between the data misfit term and the regularized term of the least-squares quadratic function should depend on the particular core parameter with respect to strength of its sensitivity profile and the level of uncertainty of its a priori information. Hence parameter specific regularization parameters are required to reflect the difference between the core parameters and how much information is contained about them in the observables' signals. This issue will be facilitated by the introduction of the full a priori covariance information about core parameters, which will be part of the future development of this project as further discussed in the next chapter.

-
1. Refer to Section 3.3.4 for the discussion on the reasons for the ill-conditioning of the operator $\bar{\bar{A}}$.
 2. Note that the uncertainty information for all core parameters is identical; that merely results in scaling the regularization parameter in Eq. (3-43) or Eq. (3-44), however for a more realistic situation, the uncertainty information is not identical, in general, for different core parameters, and that would result in an oblique projection of the type depicted in Figure 3.3.

Figure 4.2: Control Rod Pattern For Core Follow Data.
“(0/48)=Control Rod Fully Inserted/Withdrawn”

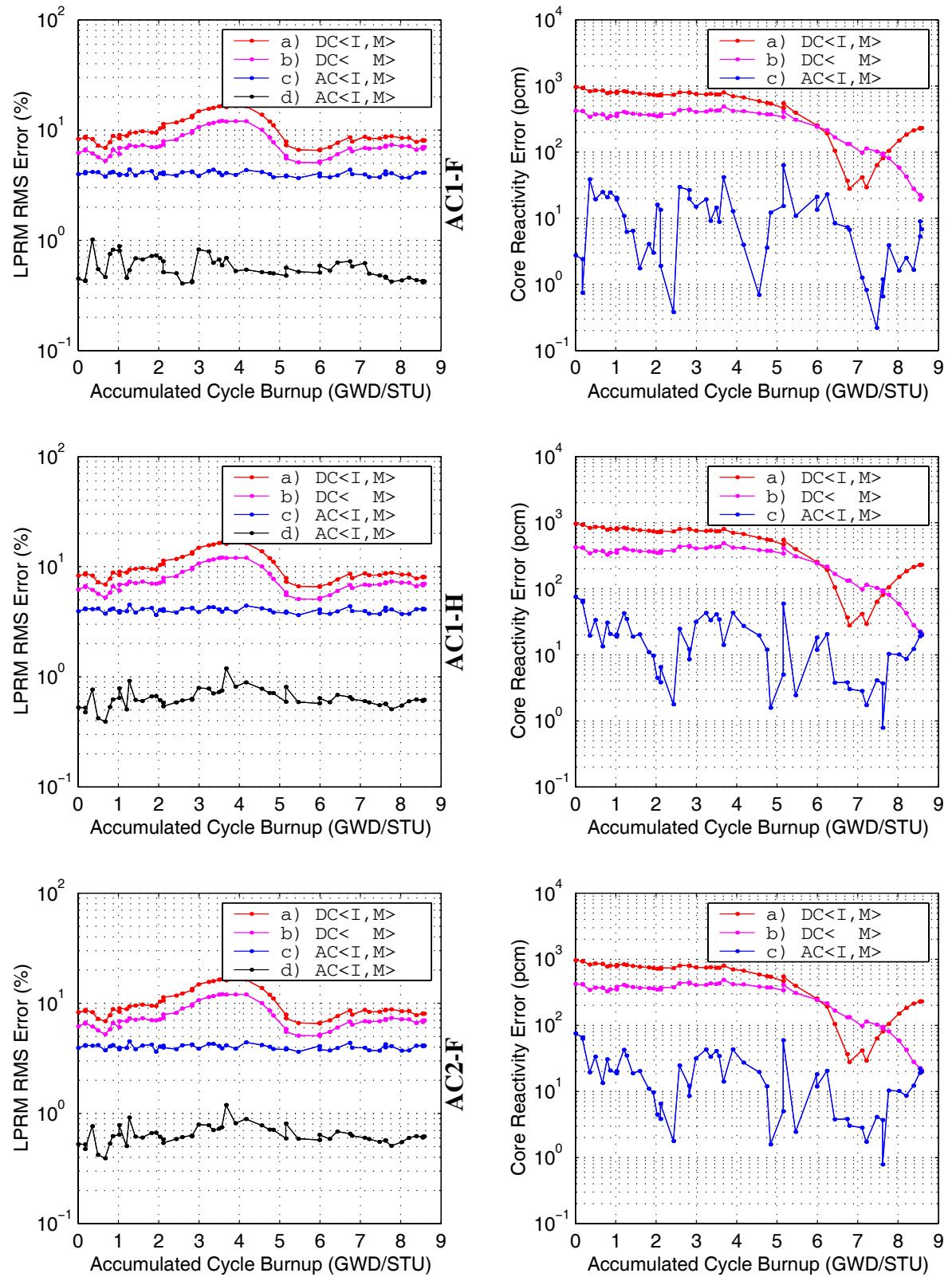


Figure 4.3: Detectors' Signals Mismatch & Core Reactivity Error (Rated Conditions).

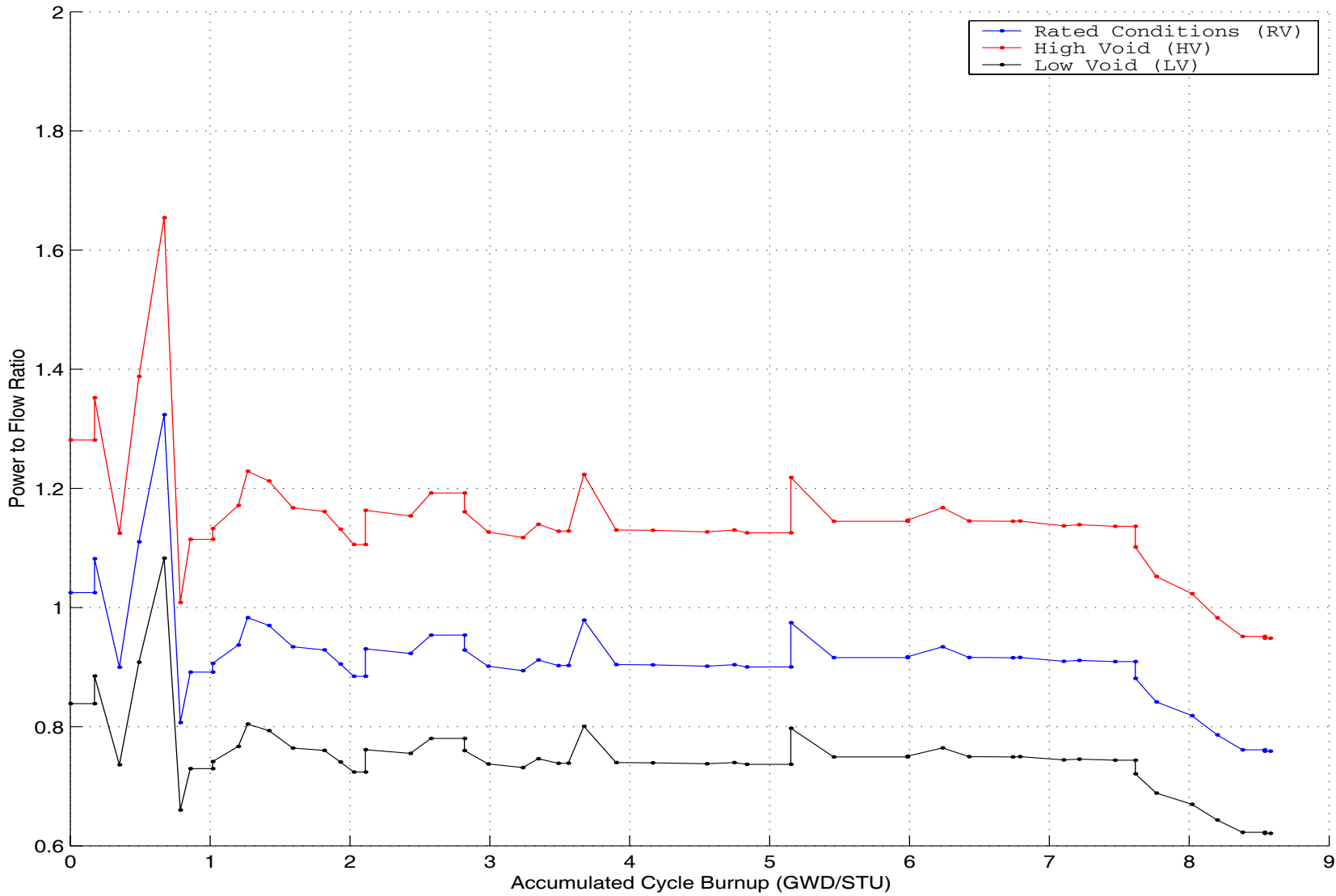
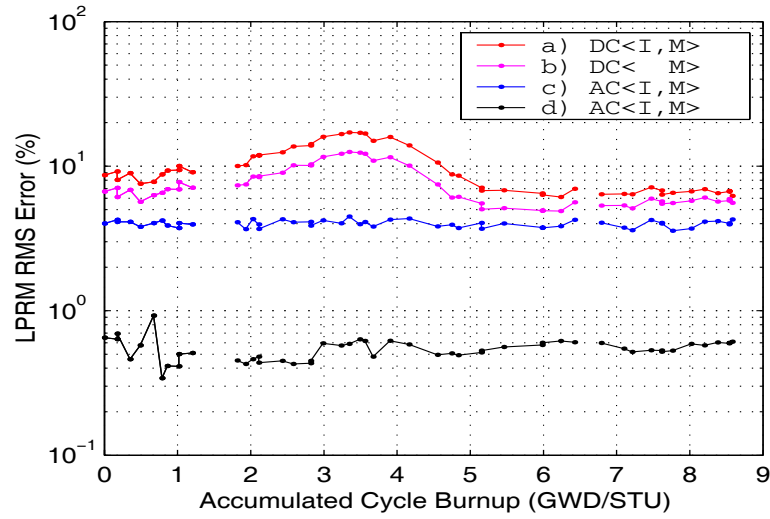
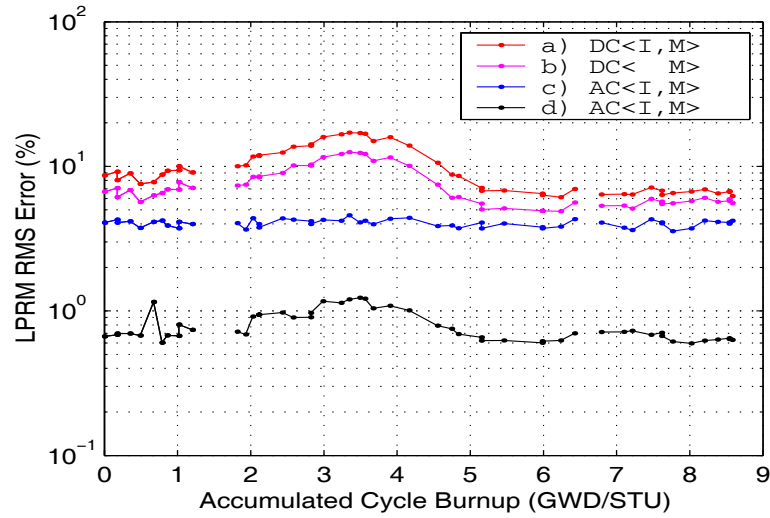
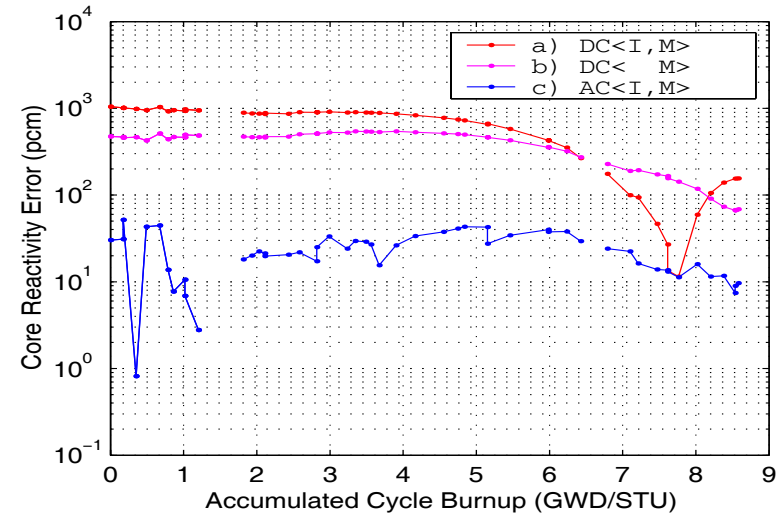


Figure 4.4: Simulated Core Follow Data at Rated Conditions, High Void and Low Void.



AC1-F



AC2-F

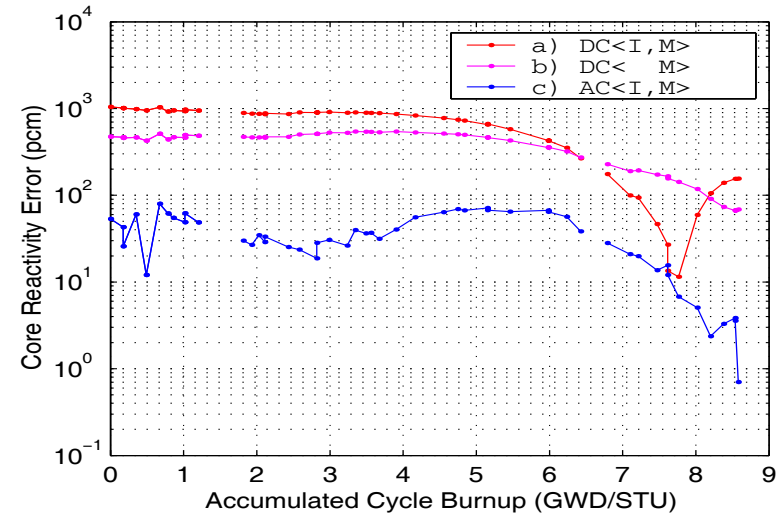
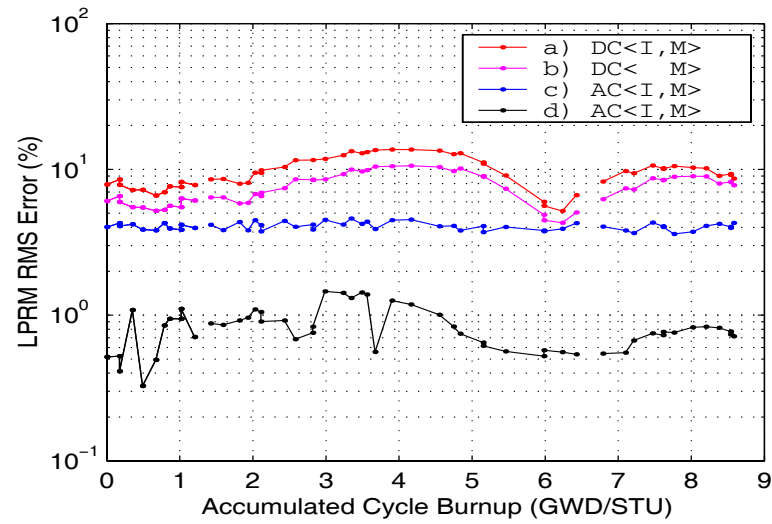
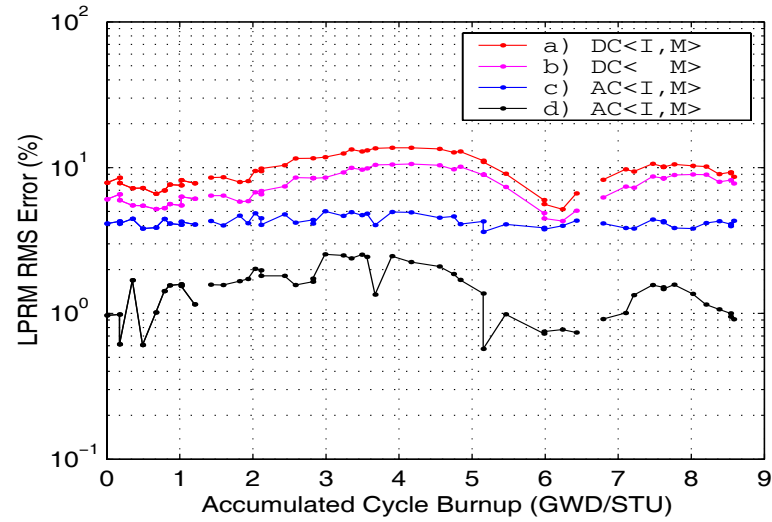
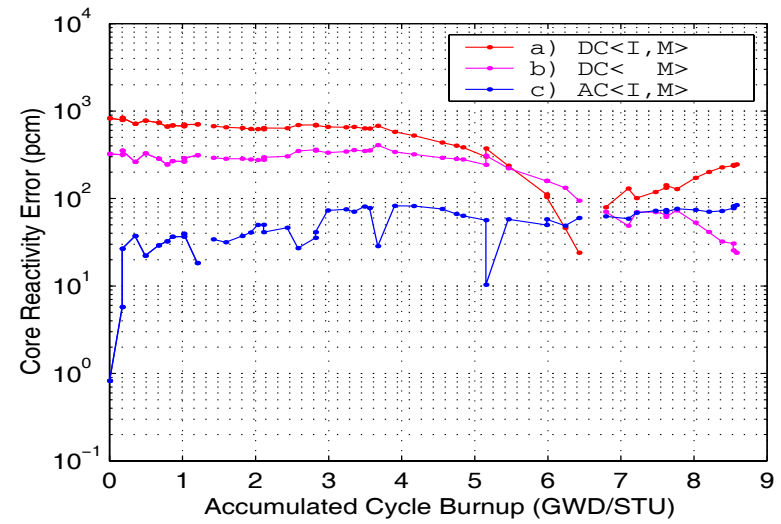


Figure 4.5: Detectors' Signals Mismatch & Core Reactivity Error (High Void Fraction).



AC1-F



AC2-F

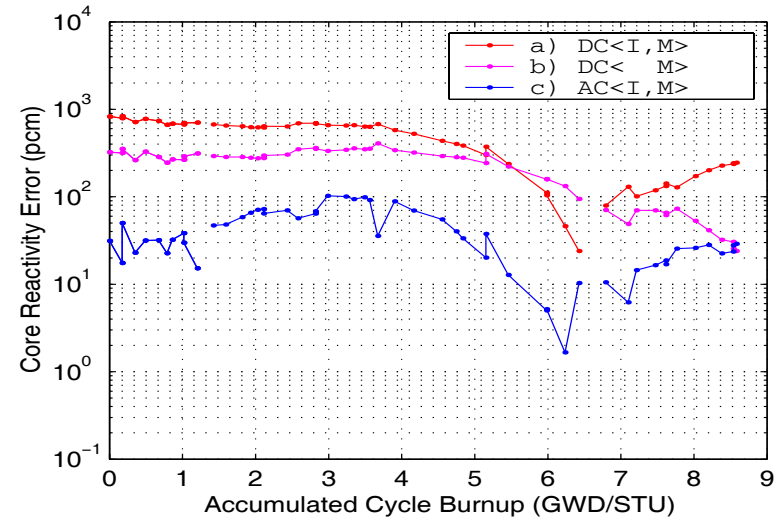


Figure 4.6: Detectors' Signals Mismatch & Core Reactivity Error (Low Void Fraction).

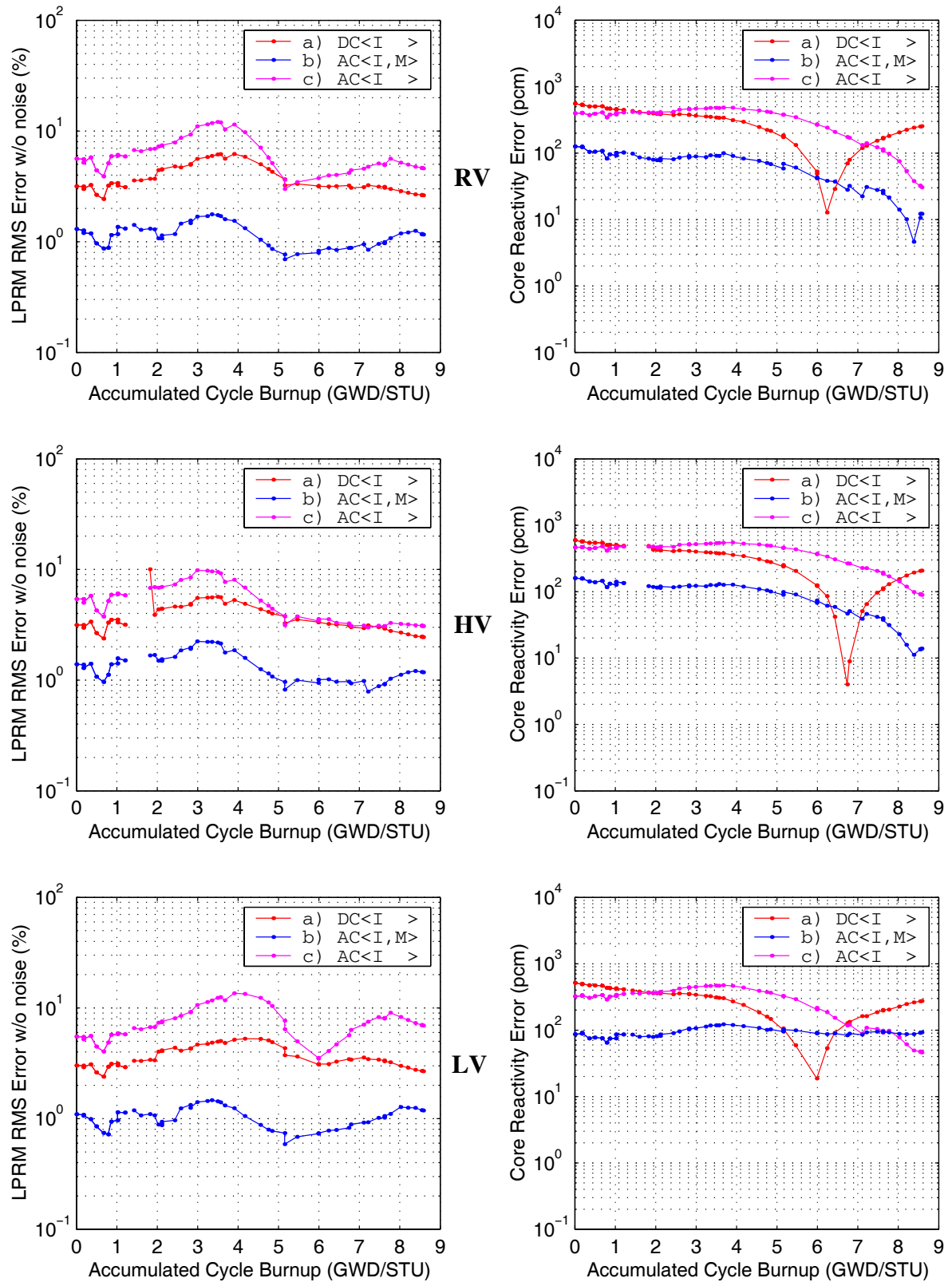


Figure 4.7: Detectors' Signals Mismatch & Core Reactivity Errors (Different Criteria).

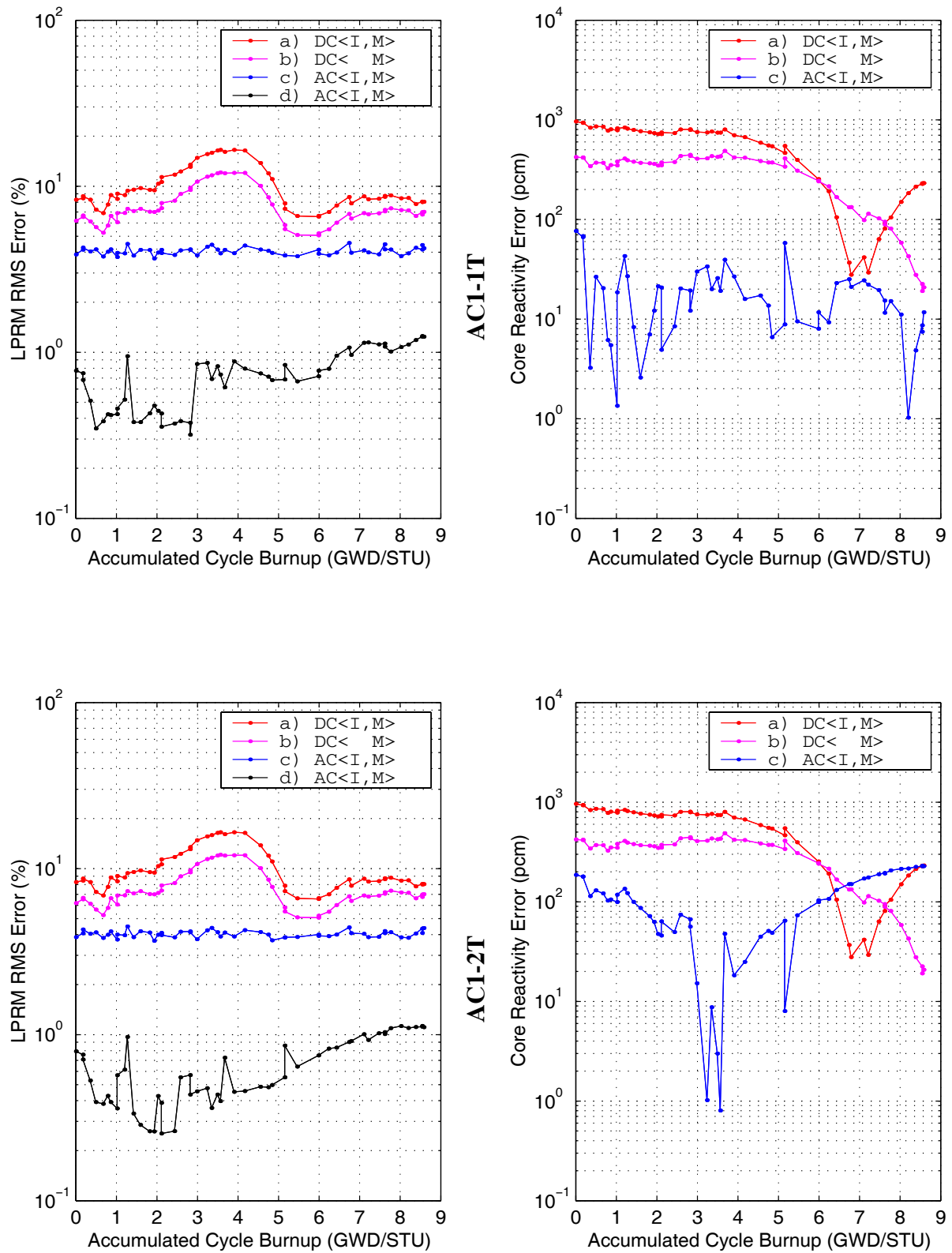


Figure 4.8: Detectors' Signal Mismatch & Core Reactivity Errors.

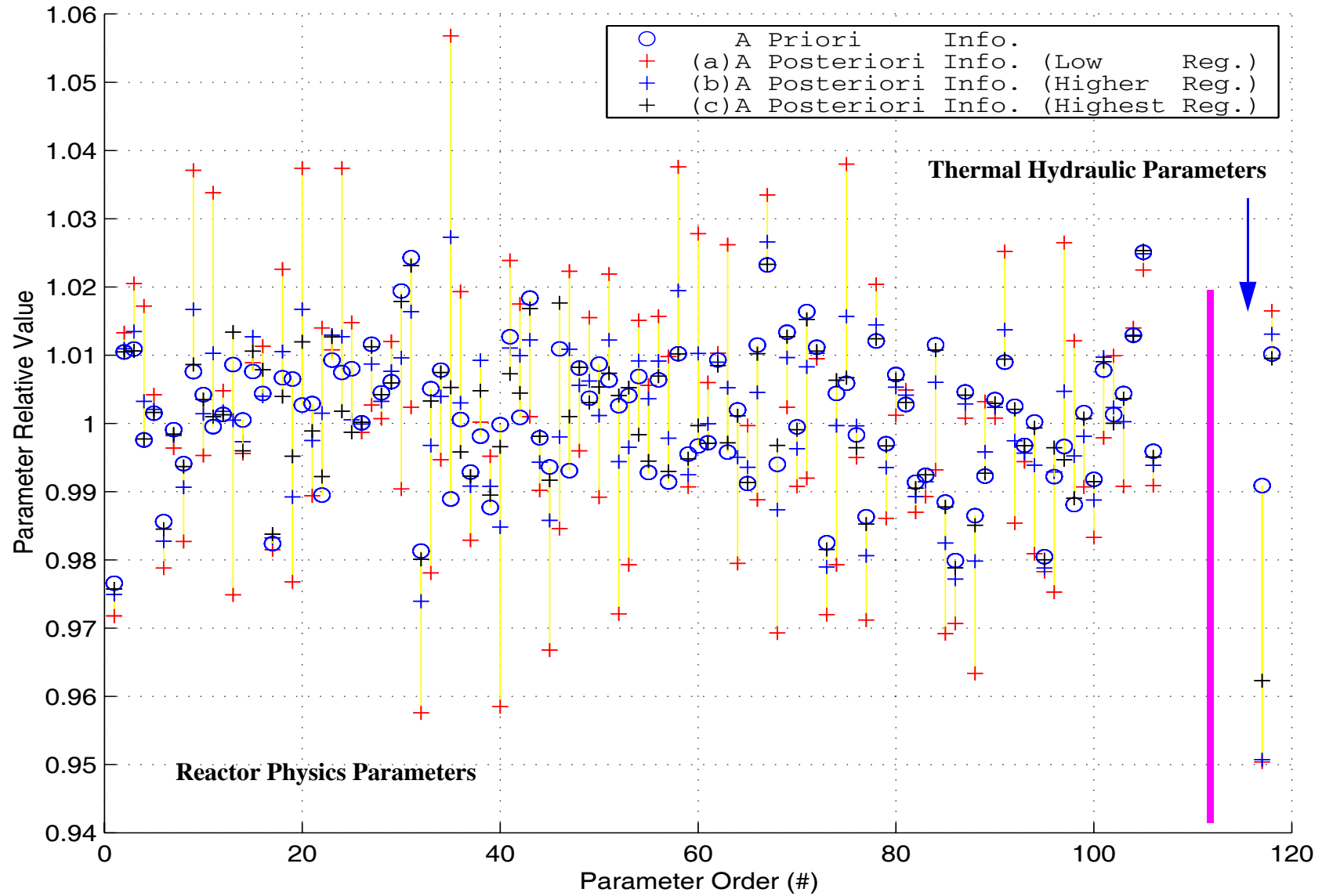


Figure 4.9: A Posteriori and A Priori Information About Model Parameters

5. Future Work and Recommendations

This study has served as a vehicle to gain insight into how effectively regularization techniques can be utilized to adapt the DC, giving rise to a meaningful adaption which is reflected in the high fidelity and robustness of the adaptive techniques employed. In these techniques, the different model parameters are adapted according to how much information about them are contained in the observables' signals. If the observables do not contain sufficient information about certain model parameters, their estimates will be confined to our best knowledge of these parameters. It was demonstrated with our choice of core parameters, we are able to separate and identify different sources of modeling or input data errors and suggest more educated guesses of error functionalization.

The observables' information content is mainly determined by sensitivity profiles of and uncertainty information on the adjusted core parameters. In the current study, sensitivity profiles were the only contributor towards the ill-conditioning nature of the adaption. Some parameters had very similar sensitivity profiles and others differed by orders of magnitude, resulting in reducing the effective rank of the least-squares associated matrix (*e.g.* the information the observables contain about the model parameters). Regularization has been performed utilizing the same regularization parameters for all adjusted core parameters. The statistical consistence between the a posteriori and a priori information about core parameters has been confirmed for a range of regularization parameters. The a posteriori uncertainty information about core parameters is determined by three factors: the a priori uncertainty about core parameters, the a priori uncertainty about core observables, and the regularization parameters (see Appendix B for more details). For this exploratory study, the uncertainty

information included in the adaption was simply modeled by diagonal covariance matrices, such that all core observables and core parameters have the same a priori uncertainty, specifically, $\sigma = 4\%$ and $\sigma = 1\%$, respectively. In reality, the full reactor physics uncertainty information has to be propagated starting from a point-wise cross-section or resonance parameters representation as available from ENDF/B and then processed through all the pre-processor codes to the core simulator. These pre-processor codes include multi-group library generation codes and lattice physics codes. To propagate the uncertainty information of the reactor physics data (*e.g.* cross-sections) from a multi-group to a few-group representation, we need the sensitivity profiles of the homogenized few-group cross-sections with respect to the multi-group cross-sections. These profiles cannot practically be obtained by a brute force technique since the number of multi-group cross-sections is huge, eliminating any chance for an effective utilization of such a simple technique. A generalized perturbation theory approach is suggested to be utilized to calculate the sensitivity profiles for both the few-group cross-sections with respect to the multi-group cross-sections and the reactor observables with respect to core parameters. This is not a trivial task to do, since the currently available lattice physics codes do not have such capability and we will have to implement it for further development of this project. The road map for the proposed project is depicted in Figure 5.1 where two paths are specifically identified. Path A propagates the uncertainty information of the reactor physics data to a few-group presentation. This path will need to be performed once for each fuel color utilized in the core under study. Path B incorporates the uncertainty information from path A with the sensitivity profiles calculated from the DC to

adapt the core model. This path will be taken repeatedly as additional core observable data becomes available.

More work will be conducted utilizing the virtual approach to better understand the capabilities of the proposed adapted techniques. For example, the virtual approach will be utilized to introduce different sources for modeling errors, specifically in thermal-hydraulics, to investigate how well the adaption can account for different and combined sources of modeling errors in the design basis core simulator. In the current work, errors are introduced in a priori information about the reactor physics core parameters utilizing a linear burnup functionalization, and the adaption is based on the same functionalization. In more realistic situations, different functionalization can be utilized in the VC and DC to gain more insight in to how well adaptive techniques will perform when error functionalization is not consistent with reality.

When the developed adaptive techniques and methodologies prove efficient and successful using the VC, actual plant data will be utilized directly to adapt existing core simulators. For this situation, the quality of the core observables (*i.e.* detector drift and failure, and deviations from steady-state, equilibrium core conditions) will need to be addressed.

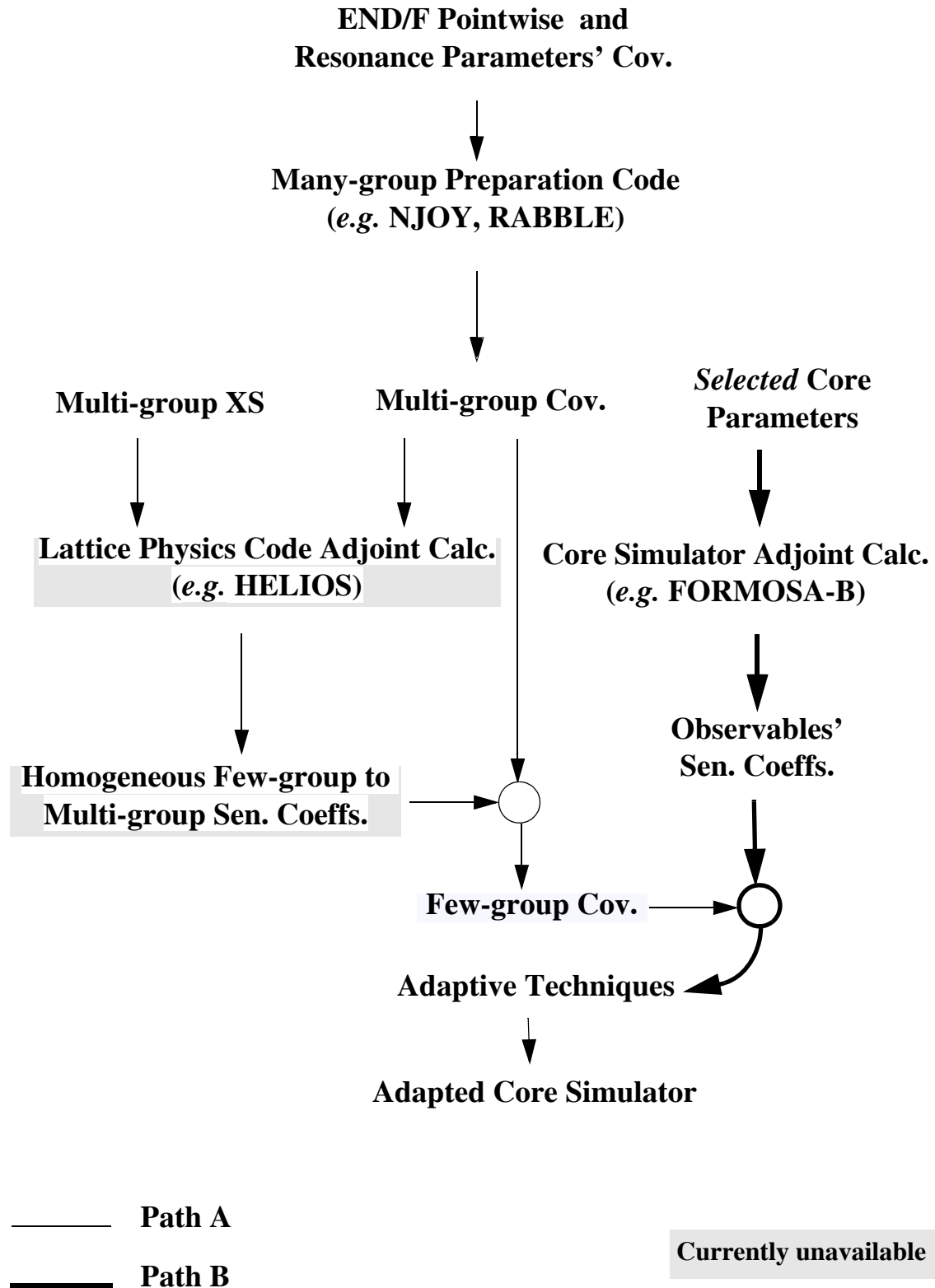


Figure 5.1: Road Map for Adaptive Core Simulation Project

References

- [1] P. Greebler, B. A. Hutchins, and C. L. Cowan, "Implications of Nuclear Data Uncertainties to Reactor Design," IAEA-CN-26/102, Second International Conference on Nuclear Data for Reactors, Helsinki, June 1970.
- [2] D. R. Harris, M. Becker, A. Paravez, and J. M. Ryskamp, "Sensitivity of Nuclear Fuel Cycle Cost to Uncertainties in Nuclear Data," *Nuclear Technology*, **46**, 82, 1979.
- [3] Hany S. Abdel-Khalik and Paul. J. Turinsky, "Inverse Method Applied to Adaptive Core Simulation," *Transactions of American Nuclear Society*, **86**, 366, 2002.
- [4] J. H. Marable, C. R. Weisbin, and G. de Saussure, "Uncertainty in the Breeding Ratio of a Large Liquid-Metal Fast Breeder Reactor: Theory and Results," *Nuclear Science and Engineering*, **75**, 30, 1980.
- [5] A. Pazy, G. Rakavy, I. Reiss, J. J. Wagschal, and Atara Ya'ari, "The Role of Integral Data in Neutron Cross-Section Evaluation," *Nuclear Science and Engineering*, **55**, 280, 1974.
- [6] C. R. Weisbin, E. M. Oblow, J. H. Marable, R. W. Peelle, and J. L. Lucius, "Application of Sensitivity and Uncertainty Methodology to Fast Reactor Integral Experiment Analysis," *Nuclear Science and Engineering*, **66**, 307-333, 1978.
- [7] Hiroshi Mitani and Hideo Kuroi, "Adjustment of Group Cross Sections by Means of Integral Data, (II)," *Journal of Nuclear Science and Technology*, **9**(11), 642, 1972.
- [8] R. W. Peelle, "Uncertainty in the Nuclear Data Used for Reactor Calculations," Advances in Nuclear Science and Technology, Vol. **14**, 1982.
- [9] J. B. Dargt, J. W. M. Dekker, H. Gruppelaar, and A. J. Janssen, "Methods of Adjustment and Error Evaluation of Neutron Capture Cross Sections; Application to Fission Product Nuclides," *Nuclear Science and Engineering*, **62**, 117, 1977.
- [10] P. J. Collins and M. J. Lineberry, "The Use of Cross Section Sensitivities in The Analysis

- of Fast Reactor Integral Parameters,” Review of The Theory and Application of Sensitivity and Uncertainty Analysis, Proceedings of a Seminar Workshop, Oak Ridge, Tennessee, ORNL/RSIC-42, 1979.
- [11] J. H. Marable and C. R. Weisbin, “Advances in Fast Reactor Sensitivity and Uncertainty Analysis,” Review of The Theory and Application of Sensitivity and Uncertainty Analysis, Proceedings of a Seminar Workshop, Oak Ridge, Tennessee, ORNL/RSIC-42, 1979.
- [12] A. N. Tikhonov, “Regularization of incorrectly posed problems,” *Soviet Mathematics Doklady*, **4**, 1624, 1963.
- [13] A. N. Tikhonov, “Solution of incorrectly formulated problems and the regularization method,” *Soviet Mathematics Doklady*, **4**, 1035, 1963.
- [14] M. Bertero and P. Boccacci, Introduction to Inverse Problems In Imaging, Institute of Physics Publishing, Bristol, 1998.
- [15] Hideo Kuroi, Hiroshi Mitani, and Kinji Koyama, “Arts and Effectiveness of Data Adjustment,” *Transactions of American Nuclear Society*, **27**, 880, 1977.
- [16] P. A. Ombrellaro, R. A. Bennett, J. W. Daughtry, R. D. Dobbin, R. A. Harris, J. V. Nelson, R. E. Peterson, and R. B. Rathrock, “Biases for current FFTF calculational methods,” Proceedings of Topical Meeting Advances in Reactor Physics, CONF-780401, Washington, D.C., 259, 1978.
- [17] Ronen, Y., Cacuci, D. G., and Wagschal, J. J., “Determination and application of generalized bias operators using an inverse perturbation approach,” *Nuclear Science and Engineering*, **77**, 426, 1981.
- [18] Fahima, W. and Ronen, Y., “The generalized bias operator method-application in two dimensional diffusion calculations,” *Transactions of Israel Nuclear Society*, **11**, 203, 1985.
- [19] Fahima, Y. and Ronen, Y., “Application of the generalized bias operator method to

- different group energy calculations,” *Transactions of Israel Nuclear Society*, **12**, 12, 1985.
- [20] Ronen, Y., “Minimization of matrices in the inverse perturbation method,” *Annals of Nuclear Energy*, **11**, 579, 1981.
- [21] William Menke, Geophysical Data Analysis: Discrete Inverse Theory, Academic Press, Inc., 1989.
- [22] A. V. Balakrishnan, Applied Functional Analysis, New York Springer, 1976.
- [23] David. G. Luenberger, Optimization by Vector Space Methods, John Wiley & Sons, Inc., 1969.
- [24] C. Nelson. Dorny, A Vector Space Approach to Models and Optimization, John Wiley & Sons, Inc. 1975.
- [25] A. N. Tikhonov, Numerical Methods for the Solution of Ill-Posed Problems, Kluwer Academic Publishers, 1995.
- [26] Heinz W. Engl, Martin Hanke, and Andreas Neubauer, Regularization of Inverse Problems, Kluwer Academic Publishers, 1996.
- [27] Jacques Hadamard, *Bull. University Princeton*, **13**, 49, 1902.
- [28] D. L. Phillips, “A Technique for the numerical solution of certain integral equations of the first kind,” *Journal of the Association for Computing Machinery*, **9**, 84, 1962.
- [29] C. W. Groetsch, The Theory of Tikhonov Regularization for Fredholm Equations of the First Kind, Pitman Advanced Pub. Program, 1984.
- [30] Brian R. Moore, Paul J. Turinsky, and Atul A. Karve, “FORMOSA-B: A Boiling Water Reactor In-core Fuel Management Optimization Package,” *Nuclear Technology*, **126**, 153, 1999.
- [31] Atul. A. Karve and Paul. J. Turinsky, “FORMOSA-B: A Boiling Water Reactor In-core Fuel Management Optimization Package II,” *Nuclear Technology*, **131**, 48, 2000.

- [32] Brian Randolph Moore, “Higher Order Generalized Perturbation Theory for BWR In-Core Nuclear Fuel Management Optimization,” PhD thesis, North Carolina State University, Department of Nuclear Engineering, Raleigh, NC, 1996.
- [33] N. Zuber and J. Findlay, “Average Volumetric Concentration in Two-Phase Flow Systems,” *Journal of Heat Transfer*, **87**, 453, 1965.
- [34] G. Lellouche and B. Zolotar, Mechanistic Model for Predicting Two-Phase Void Fraction in Vertical Tubes, Channels, and Rod Bundles, EPRI NP-2246-SR (1982).
- [35] “FORMOSA-B Microscopic Cross Section Model Development”, EPRC Annual Report 2001.
- [36] Albert Tarantola, Inverse Problem Theory, Methods for Data Fitting and Model Parameter Estimation, Elsevier Science Publishers B. V., 1987.
- [37] Carl. D. Meyer, Matrix Analysis and Applied Linear Algebra, Society for Industrial and Applied Mathematics, 2000.
- [38] S. M. Tan and C. Fox, Inverse Problems 453.707 classnotes, The University of Auckland, Auckland, New Zealand., 2001.
- [39] R. Richardson, Inverse Problems In Geophysics, Geosciences 567, The University of Arizona., 2001.
- [40] Ed Soares, Inverse Problems Math202, College of Holy Cross., 2001.
- [41] Charles L. Lawson and Richard J. Hanson, Solving Least Squares Problems, Prentice-Hall, Inc., Englewood Cliffs, N. J., 1974.
- [42] Albert Tarantola and Bernard Valette, “Generalized Nonlinear Inverse Problems Solved Using the Least Squares Criterion,” *Reviews of Geophysics Space Physics*, **20-2**, May 1982.
- [43] Yigal Ronen, Uncertainty Analysis, CRC Press Inc., 1988.

- [44] B. L. Broadhead, C. M. Hopper, R. L. Childs, and C. V. Parks, "Sensitivity and Uncertainty Analyses Applied to Criticality Safety Validation," *Oak Ridge National Laboratory*, ORNL/TM-13692/V1, NUREG/CR-6655, VOL. 1, November 1999.
- [45] Netlib Repository <http://www.netlib.org>, LAPACK Driver routines.

Appendices

A. Data Information Content

A forward problem can be viewed as one in which information content about the model parameters is reduced due to transformation from the parameters space to the data space. Consider the following example to demonstrate a qualitative explanation of the concept of data information content[14]. For a transient one dimensional heat conduction problem, the forward problem can be formulated as follows

$$\frac{\partial^2 T}{\partial x^2} = \frac{1}{\alpha} \frac{\partial T}{\partial t} \quad (\text{A-1})$$

where T is the temperature, α is the thermal diffusivity, and the initial and boundary conditions are given as follows:

$$T(x, 0) = \theta(x); \quad T(0, t) = T(a, t) = 0. \quad (\text{A-2})$$

The problem can be solved by Fourier expansion,

$$T(x, t) = \sum_{n=1}^{\infty} T_n(t) \sin\left(\pi n \frac{x}{a}\right) \quad (\text{A-3})$$

and the solution is

$$T_n(t) = \theta_n e^{-\alpha \left(\pi \frac{n}{a}\right)^2 t} \quad (\text{A-4})$$

where θ_n is determined to satisfy the initial conditions, *i.e.*

$$\theta(x) = \sum_{n=1}^{\infty} \theta_n \sin\left(\pi n \frac{x}{a}\right) \quad (\text{A-5})$$

Assume that the input data $\theta(x)$ are known within a certain degree of accuracy ε . It follows that only the first N_0 terms which satisfy $\theta_n > \varepsilon$ are to be considered. Since each component

in T , (e.g. T_n), is the same as the corresponding component in θ , (e.g. θ_n), but damped by an exponential factor, this means that the number of terms N_T for which $T_n > \varepsilon$ will be much less than N_θ , (i.e. $N_T < N_\theta$); in other words the information content of the data space is less than that of the parameters space. Another issue to be noted here, if we were to predict $T(x, t)$ at earlier times from information at $t > t_0$, this will simply result in magnifying the Fourier coefficients $\{\theta_n\}$ by the exponential term. This means, if there is any higher order noise imposed on the data, it will be magnified dramatically, giving rise to an unphysical behaviour prediction.

B. Tikhonov Regularization

Tikhonov regularization[12]-[13] is the most common regularization technique, sometimes called Tikhonov-Phillips[28] regularization. A brief demonstrative discussion of this regularization technique for the discrete inverse problem is presented in this appendix. Refer to Eq. (3-42) and consider a general case where the a priori information are represented by the vector nonlinear equation,

$$\vec{\Phi}(\bar{p}_\infty) = \vec{\Phi}_\infty, \quad (0-1)$$

where $\vec{\Phi}_\infty \in R^s$. That formula can be linearized around a reference point according to,

$$\vec{\Phi}(\bar{p}) = \vec{\Phi}(\bar{p}_0) + \bar{L}(\bar{p} - \bar{p}_0) + \text{Higher order terms}, \quad (0-2)$$

where the Jacobian matrix \bar{L} is defined by,

$$[\bar{L}]_{ij} = \frac{\partial}{\partial \bar{p}_{0j}} \vec{\Phi}_i(\bar{p}_\infty), \quad (0-3)$$

with $\bar{L} \in R^{s \times n}$. Let $\bar{p}_0 = \bar{p}_{k-1}$ be the current iterate value. The search for the new iterate \bar{p}_k

can be found by minimizing the quadratic form¹,

$$S(\bar{d}_k^c, \bar{p}_k) = \min_{\bar{p}_k} \left\{ \|\bar{d}^m - \bar{d}_k^c\|^2 + \mu^2 \|\vec{\Phi}_\infty - \vec{\Phi}(\bar{p}_{k-1})\|^2 \right\} \quad (0-4)$$

subject to:

$$\bar{d}_k^c = \bar{d}_{k-1}^c + \bar{A}(\bar{p}_k - \bar{p}_{k-1}) \quad (0-5)$$

1. Discussion is limited to the unconstrained minimization problem.

where \vec{d}^m and \vec{d}_k^c denote the measured and predicted observables, respectively. Eq. (0-5) can be re-written as,

$$S(\bar{p}_k) = \min_{\bar{p}_k} \left\{ \left\| \Delta \vec{d}_k^m - \bar{A} \Delta \bar{p}_k \right\|^2 + \mu^2 \left\| \bar{L} \Delta \bar{p}_k - \Delta \vec{\Phi}_{\infty k} \right\|^2 \right\}, \quad (0-6)$$

where $\Delta \vec{\Phi}_{\infty k} = \vec{\Phi}_{\infty} - \vec{\Phi}(\bar{p}_{k-1})$ and the other “ Δ ” terms meanings are obvious. The first term on the R.H.S. is referred to as the data misfit term, and the second term is the regularized term. Eq. (0-6) is equivalent to requiring that

$$\begin{bmatrix} \bar{A} \\ \mu \bar{L} \end{bmatrix} \Delta \bar{p}_k = \begin{bmatrix} \Delta \vec{d}_k^m \\ \mu \Delta \vec{\Phi}_{\infty k} \end{bmatrix} \quad (0-7)$$

be satisfied, in a least-squares sense.

Assuming that \bar{L} has a full column rank, the least-squares solution is obtained by projecting the R.H.S. on the range of the matrix operator $\begin{bmatrix} \bar{A}^T & \mu \bar{L}^T \end{bmatrix}^T$. This is achieved by multiplying both sides by the transpose of this matrix operator¹.

$$\begin{aligned} \begin{bmatrix} \bar{A}^T & \mu \bar{L}^T \end{bmatrix} \begin{bmatrix} \bar{A} \\ \mu \bar{L} \end{bmatrix} \Delta \bar{p}_k &= \begin{bmatrix} \bar{A}^T & \mu \bar{L}^T \end{bmatrix} \begin{bmatrix} \Delta \vec{d}_k^m \\ \mu \Delta \vec{\Phi}_{\infty k} \end{bmatrix} \\ \therefore (\bar{A}^T \bar{A} + \mu^2 \bar{L}^T \bar{L}) \Delta \bar{p}_k &= \bar{A}^T \Delta \vec{d}_k^m + \mu^2 \bar{L}^T \Delta \vec{\Phi}_{\infty k}, \\ \therefore \Delta \bar{p}_k &= (\bar{A}^T \bar{A} + \mu^2 \bar{L}^T \bar{L})^{-1} (\bar{A}^T \Delta \vec{d}_k^m + \mu^2 \bar{L}^T \Delta \vec{\Phi}_{\infty k}) \end{aligned} \quad (0-8)$$

1. Refer to Eq. (3-14) for justification.

where μ is a regularization parameter. As a first crude approach, assume that $\bar{\bar{L}} = \bar{\bar{I}}$ is the identity matrix (*i.e.* $\bar{\bar{\Phi}}(\bar{p}_\infty) = \bar{p}_\infty$); it is easy to show that¹,

$$\Delta \bar{p}_k = \sum_{i=1}^n [\Delta \dot{\bar{p}}_k]_i \bar{v}_i, \quad (0-9)$$

where $\{[\Delta \dot{\bar{p}}_k]_i\}$ are given by,

$$[\Delta \dot{\bar{p}}_k]_i = \frac{\sigma_i [\Delta \dot{\bar{d}}_k^m]_i + \mu^2 [\bar{p}_\infty - \bar{p}_{k-1}]_i}{\sigma_i^2 + \mu^2}, \quad (0-10)$$

where $\{\sigma_i\}$ denote the singular values of $\bar{\bar{A}}$. Regularization can be visualized as a filter. It is

easy to show that the condition number of the matrix $(\bar{\bar{A}}^T \bar{\bar{A}} + \mu^2 \bar{\bar{I}})$ is given by:

$$K = \frac{\sigma_{max}^2 + \mu^2}{\sigma_{min}^2 + \mu^2}. \quad (0-11)$$

Figure B.2 plots on a logarithmic scale the condition number of the matrix $\bar{\bar{A}}^T \bar{\bar{A}} + \mu^2 \bar{\bar{I}}$ against different regularization parameters.

For those pieces of information $[\Delta \dot{\bar{d}}_k^m]_i$ that have small singular values associated with them (*i.e.* $\sigma_i^2 \ll \mu^2$), the a priori information is utilized instead of the observables ($[\Delta \dot{\bar{d}}_k^m]_i$) to estimate the corresponding components of the model parameters ($[\Delta \dot{\bar{p}}_k]_i$). If $\mu^2 \rightarrow 0$, then $[\Delta \dot{\bar{p}}_k]_i \rightarrow [\Delta \dot{\bar{d}}_k^m]_i / \sigma_i$; the problem reduces to a regular least-squares problem (see Eq. (3-

1. Refer to Eq. (3-16) for comparison.

16)); whereas, if $\mu^2 \rightarrow \infty$, then $[\Delta \bar{p}]_i \rightarrow [\bar{p}_\infty - \bar{p}_{k-1}]_i$; the data misfit term is negligible with respect to the regularized term, and the solution is mainly determined by the a priori information.

The relation between the a priori and a posteriori information about model parameters and the corresponding core observables is described by the L-curve. Figure B.1 shows that for a very small regularization parameter, the best fit is obtained (*i.e.* the best agreement between the measured and predicted observables); however, the estimates for the model parameters are very far (in terms of the norm $\|\bar{p}_k - \bar{p}_\infty\|$) from our best knowledge (a priori information). For large regularization parameters, the worst agreement is obtained, that corresponds to the initial discrepancies which exist between the actual plant data and the predictions of an existing core

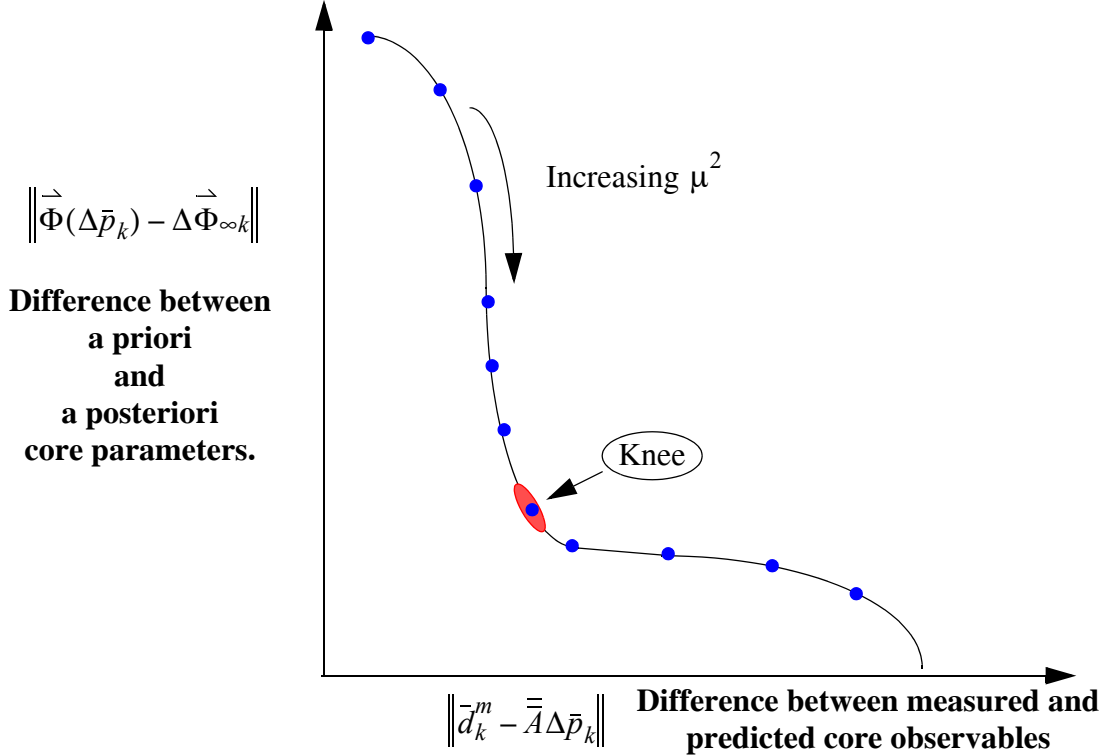


Figure B.1: L-Curve, ‘A Posteriori Information about Model Parameters and Core Observables’.

simulator (*i.e.* between the virtual and design basis core simulators for our virtual approach). The L-curve suggests that when one increases the regularization parameters gradually, there is a region where the quality of the data misfit stays the same; while the agreement between the a posteriori and a priori information about model parameters increases considerably. A knee-type behaviour is depicted in the figure, where in this region, the agreement between the adapted design core and the actual plant data starts to degrade without any significant change in the model parameters. That behaviour suggests that one should select a regularization parameters at the knee region of the L-curve. In this region, one would obtain the best agreement between the predicted and measured observables and at the same time, the adaption is restricted to the best a priori information about model parameters; hence giving rise to a physical adaption. The L-curve has been reproduced in Figure B.3, for illustration purposes, for an iterate k during an unconstrained search for model parameters. The knee-type behaviour is easily identified in the curve. In our work, more than one regularization parameters has been utilized, and their optimum values were obtained by trial and error.

Referring to Eq. (0-10), one can see how the a priori uncertainty about core parameters and observables propagate through the adaptive techniques and appear in the a posteriori uncertainty information about core parameters. It is easy to show that,

$$\delta[\Delta\dot{\bar{p}}_k]_i = \frac{\sigma_i \delta[\Delta\dot{\bar{d}}_k^m]_i + \mu^2 \delta[\bar{p}_\infty - \bar{p}_{k-1}]_i}{\sigma_i^2 + \mu^2}, \quad (3-12)$$

where $\delta[x]$ is the uncertainty component associated with x . Note that when the regularization parameters approaches zero, the uncertainty in the a posteriori information is given by,

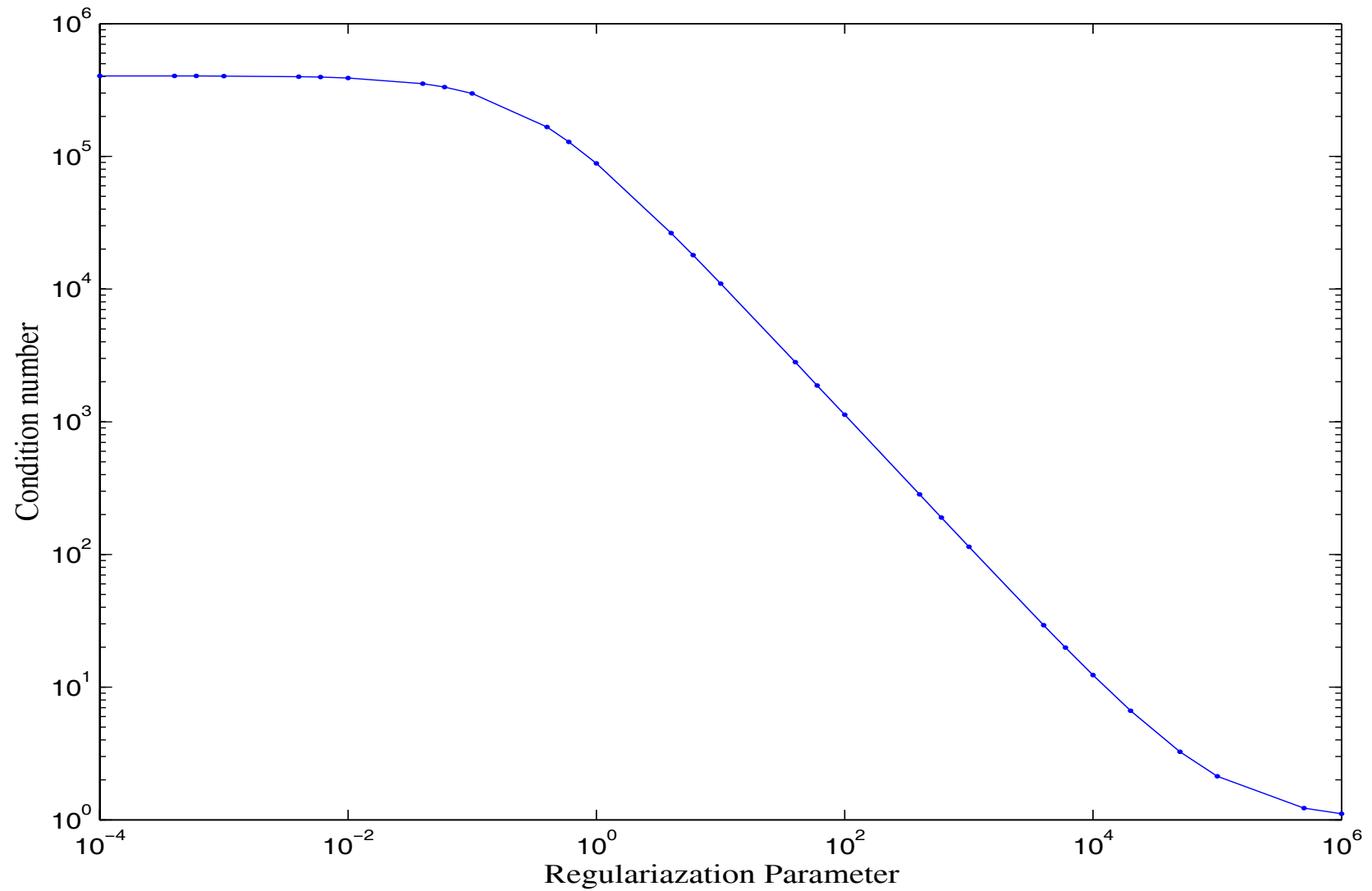


Figure B.2: Effect of Regularization on the Conditioning of the Unconstrained Least-Squares Problem

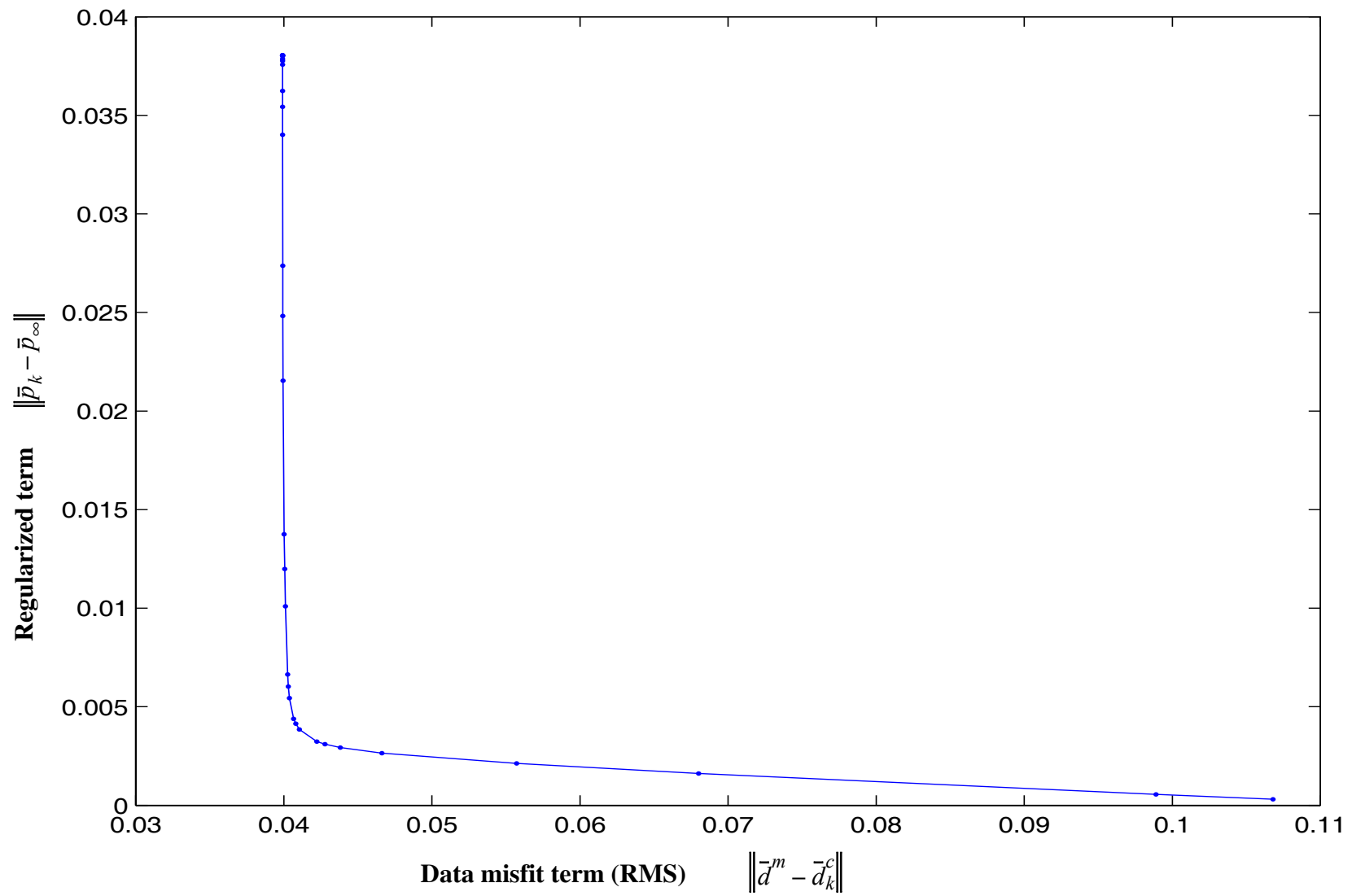


Figure B.3: L-Curve for a Single Iteration Unconstrained Search

$$\delta[\Delta\dot{\bar{p}}_k]_i \rightarrow \frac{\delta[\Delta\dot{\bar{d}}_k^m]_i}{\sigma_i}.$$

This is an undesirable situation since for the particular component $\delta[\Delta\dot{\bar{p}}_k]_i$, when the associated singular value σ_i is very small, that results in magnifying the error component of the observables, $\delta[\Delta\dot{\bar{d}}_k^m]_i$. On the other hand, when the regularization parameter approaches infinity,

$$\delta[\Delta\dot{\bar{p}}_k]_i \rightarrow \delta[\bar{p}_\infty - \bar{p}_{k-1}]_i$$

(*i.e.* the a posteriori uncertainty information approaches the a priori uncertainty). For those components $\delta[\Delta\dot{\bar{p}}_k]_i$ whose associated singular values are relatively large, the a posteriori uncertainty can be made to be less than the a priori uncertainty. Hence, it is undesirable to have a large regularization parameter since that will increase the a posteriori uncertainty about those components of core parameters. This shows that it would be beneficial to include regularization parameters which are component-wise dependent. In the current work, the a priori uncertainty about model parameters is identical for all core parameters (*i.e.* 1% standard deviation). It is easy to show that this is equivalent to scaling the regularization parameters¹ (*i.e.* the same regularization parameters are utilized for all estimated components in Eq. (3-12)). In a realistic situation, inclusion of the a priori uncertainty, represented by a covariance matrix, will effectively give rise to regularization which is component-wise dependent.

1. Refer to section 3.2.13.